AD-A163 996

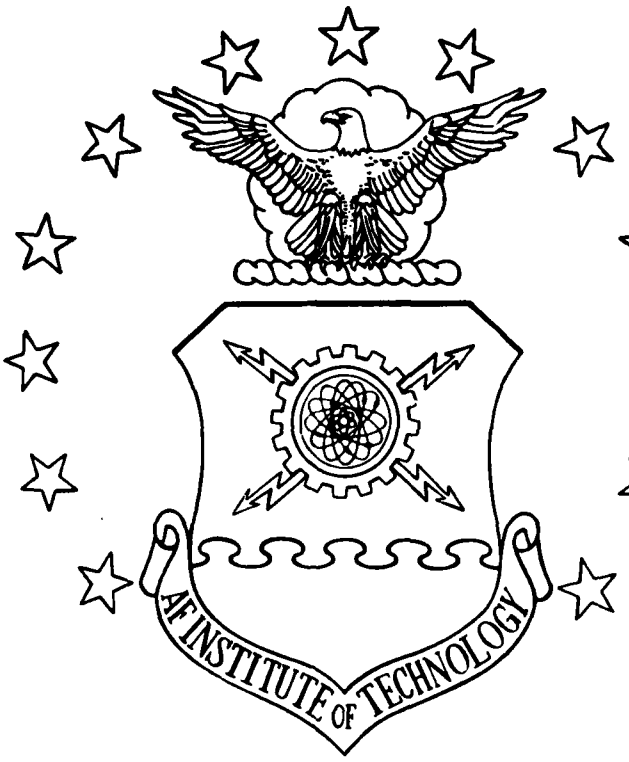

DTIC
ELECTE
FEB 1 3 1986
S D
D

MINIMUM IMPULSE

ORBITAL EVASIVE MANEUVERS

THESIS

Roger C. Burk
Captain, USAF

AFIT/GSO/AA/85D-3

DTIC FILE COPY

DEPARTMENT OF THE AIR FORCE
AIR UNIVERSITY
AIR FORCE INSTITUTE OF TECHNOLOGY

Wright-Patterson Air Force Base, Ohio

86 2 12 039

AFIT/GSO/AA/85D-3

DTIC
ELECTE
FEB 1 3 1986
S D
D

MINIMUM IMPULSE

ORBITAL EVASIVE MANEUVERS

THESIS

Roger C. Burk
Captain, USAF

AFIT/GSO/AA/85D-3

Approved for public release; distribution unlimited

AFIT/GSO/AA/85D-3

MINIMUM IMPULSE ORBITAL EVASIVE MANEUVERS

THESIS

Presented to the Faculty of the School of Engineering

of the Air Force Institute of Technology

Air University

In Partial Fulfillment of the

Requirements for the Degree of

Master of Science in Space Operations

Roger C. Burk, A.B.

Captain, USAF

December 1985

Accesion For

NTIS CRA&I ☑
DTIC TAB ☐
Unannounced ☐
Justification .....

By .....
Distribution /

Availability Codes

Dist	Avail and / or Special
A-1	

Approved for public release; distribution unlimited

Preface

I began this research with the goal in mind of creating a computer program that could be used tactically to find the best evasive maneuver for a given satellite under a given attack. I was able to make substantial progress, and I believe that a tactically useful program is not too far away.

One problem that took a good deal of time was the calculation of the matrix $\underset{\sim}{\Phi}$, the matrix of partial derivatives of an orbital state vector at one time with respect to the vector at an earlier time. The calculation is of no theoretical interest, but it is included in Section III in the hopes that future students can be spared this painstaking drudgery.

I owe the usual thanks for helpful assistance to my faculty advisor, Lt Col Joseph W. Widhalm, along with greater than usual thanks for the confidence he showed in me and the freedom he gave me to develop the project in my own way.

Roger C. Burk

Table of Contents

		page
Preface		ii
List of Figures		v
List of Tables		vi
Abstract		vii
I.	Introduction	1-1
II.	Analytical Development	2-1
	Mathematical Model of an Orbital Interception	2-1
	Optimal Trajectory to the Threat Sphere	2-4
	Optimal Trajectory Tangent to the Threat Sphere	2-10
	Allowing Time of Flight to Vary	2-15
	The Moving Attacker	2-18
III.	Computer Implementation	3-1
	General Description	3-1
	Generating the Phi Matrix	3-2
	Convergence Criteria	3-8
	Finding Multiple Solutions	3-9
	Ruling Out a Second Close Approach	3-10
IV.	Limitations and Numerical Problems	4-1
	Astrodynamic Model	4-1
	Extreme Orbits	4-1
	Very Early Maneuvers and Multiple Revolutions	4-3
	Choice of Coordinate Axes	4-3
	Singularities and Overflows	4-4
	Speed of Convergence	4-5

V. Results 5-1

Sample Input and Output 5-1
Maneuvers 12 Hours before a Geosynchronous Interception 5-5
Maneuvers 6 Hours before a Geosynchronous Interception 5-10
Minimum Energy Geosynchronous Interception 5-11
A Standard Interception 5-12
Variations on the Standard 5-14

VI. Conclusions 6-1

Factor that Affect Maneuver Size 6-1
Tactics 6-2
Suggestions for Further Work 6-4

Appendix: Tabulated Results for Variations on the Standard Interception A-1

Bibliography BIB-1

Vita VITA-1

List of Figures

Figure		Page
2.1.	Evasive Trajectories	2-3
2.2.	Tangent Trajectories to Concentric Spheres . .	2-11
4.1.	Iterations vs. Maneuver Interval	4-6
4.2.	Locus of Trajectory End Points	4-7
4.3.	Factors Used for Short Maneuver Intervals . .	4-9
5.1.	Sample Program Input	5-2
5.2.	Sample Program Output	5-4
5.3.	12-hour Geosynchronous Maneuver	5-5
5.4.	Tangent Ellipses with Varying Flight Times . .	5-8
5.5.	Impulse vs. Threat Sphere Radius	5-16
5.6.	Impulse vs. Short Maneuver Intervals	5-17
5.7.	Impulse vs. Long Maneuver Intervals	5-18
5.8.	Impulse vs. Attacker Speed	5-20
5.9.	Impulse vs. Attacker Orbital Inclination . . .	5-21
5.10.	Impulse vs. Attacker Flight Path Angle	5-22
5.11.	Impulse vs. Satellite Speed	5-24
5.12.	Impulse vs. Satellite Flight Path Angle . . .	5-25
5.13.	Impulse vs. Satellite Orbital Altitude	5-27
5.14.	Impulse vs. Intercept Radial Miss Distance . .	5-28
5.15.	Impulse vs. Intercept In-track Miss Distance .	5-29
5.16.	Impulse vs. Intercept Cross-track Miss Distance	5-31

List of Tables

Table		Page
5.1.	No Tangency, Fixed Time, Fixed Threat	5-6
5.2.	Tangency, Fixed Time, Fixed Threat	5-7
5.3.	Tangency, Varying Time, Fixed Threat	5-7
5.4.	Tangency, Varying Time, Moving Threat	5-9
5.5.	6 Hour Interval, Fixed Threat	5-10
5.6.	6 Hour Interval, Moving Threat	5-11
5.7.	Summary of Geosynchronous Orbit Cases	5-13
5.8.	Summary of Variations on the Standard Interception	5-32
A.1.	Minimum Evasive Impulse vs. Threat Sphere Radius	A-2
A.2.	Minimum Evasive Impulse vs. Maneuver Interval	A-2
A.3.	Minimum Evasive Impulse vs. Attacker Speed . .	A-3
A.4.	Minimum Evasive Impulse vs. Attacker Orbital Inclination	A-3
A.5.	Minimum Evasive Impulse vs. Attacker Flight Path Angle	A-4
A.6.	Minimum Evasive Impulse vs. Satellite Speed .	A-4
A.7.	Minimum Evasive Impulse vs. Satellite Flight Path Angle	A-5
A.8.	Minimum Evasive Impulse vs. Satellite Orbit Radius	A-5
A.9.	Minimum Evasive Impulse vs. Intercept Radial Miss Distance	A-6
A.10.	Minimum Evasive Impulse vs. Intercept In-track Miss Distance	A-6
A.11.	Minimum Evasive Impulse vs. Intercept Cross-track Miss Distance	A-6

Abstract

A threat to a satellite is modeled as a sphere of given radius. The satellite may be required to be outside of the sphere at a given time or never to enter the sphere at all. The threat sphere may be inertially fixed or may move in a keplerian orbit. A method is developed of finding the smallest impulsive maneuver that can be made at a given time to avoid the threat. Using the linearized relationship between the satellite state vector at the maneuver time and the state at the intercept time, iterative algorithms are developed that converge on the optimal evasive maneuver. A computer program that implements the algorithms is described. The results of the algorithms are given for several cases. An interception taken from a plausible real-world scenario is used as a basis for investigating how maneuver size varies with the geometry of the interception.

MINIMUM IMPULSE ORBITAL EVASIVE MANEUVERS

I. Introduction

Much research is being done on the astrodynamics of orbital transfer and rendezvous, but there is nothing in the recent open literature on the problem of avoiding an interception in space. Until recently the problem has not been of great practical interest. However, more and more military capabilities are being put in satellites and the means of intercepting them are improving. Some research has been done on optimal interception (3). The problem of avoiding an interception also needs attention. The simplest way to defeat an interception is to maneuver the attacked satellite so that it does not come within the lethal radius of the attacker. However, any orbital maneuver will use up the satellite's limited supply of propellant, perhaps shortening its useful life or leaving it vulnerable to a second attack. All other things being equal, the evasive maneuver should be as small as possible. This thesis develops algorithms that can be used to calculate the smallest impulsive maneuver that will evade a given attempt at orbital interception.

The mathematical method used was to find the linear small-value approximation for the relationship between changes in velocity at the time of maneuver and changes in

position and velocity at the time of interception. Analysis of this relationship gave an approximate answer for the optimal evasive maneuver, and successive iterations refined the answer to the desired accuracy. Another approach explored was to express the maneuver as a function of the orbital parameters of the evasive trajectory, starting with the formulas in Section 7.4 of Kaplan (2:308-329). The minimum of the function would then be found with standard numerical analysis software. This second approach was eventually dropped in favor of the first. The writer was more familiar with the iterative method, it was computationally simpler, and it seemed to offer greater flexibility in changing the constraints of the problem.

This thesis contains all the mathematical analysis in Section II, a description of the computer implementation of the algorithms in Sections III and IV, and the results of the computer program in Section V. In Section II, the problem is described mathematically. An algorithm is then developed that converges on an optimal maneuver that puts the satellite at a given distance from the threat at a given time. Then an additional constraint is imposed on the problem: at the given time the approach rate of the threat must vanish, so that the threat is never closer than the given distance. Algorithms are developed for this case, both with the time of closest approach fixed and with it allowed to vary. Up to this point the threat was considered to be fixed in inertial space; the final step is

to consider a threat that is moving in an orbit of its own. Modifying the algorithm to account for this completes the mathematical analysis of the problem.

Once the analysis was complete, the next task was to write a computer program to do the calculations. Section III tells how this job was approached. A general description of the program is given and the astrodynamic model used is described. Criteria are established for determining when convergence occurs. Since the algorithms can guarantee only that a certain maneuver is locally optimal, i.e. that it is better than any similar but slightly different maneuver, a procedure for finding the globally optimal maneuver had to be developed. This method is presented, followed by the calculations used to assure that the evasive trajectories in fact never come closer to the threat than is desired.

Section IV describes certain limitations of the computer program used and some numerical problems encountered. The limits of the astrodynamic model are discussed. The behavior of the program with very eccentric or hyperbolic orbits and with very long spans of time is described. The effect of the choice of coordinate axes is discussed and some remarks are made on numerical singularities and floating point overflows during computation. Finally, the speed of convergence of the algorithms is examined in some detail, for this was found to be a major problem. In most cases the program converged quite promptly, but in certain

intercept geometries, and whenever time between maneuver and interception became short or the size of the orbit became very large, convergence became extraordinarily slow. How this problem was overcome is presented.

The program's results are introduced with a description of its inputs and outputs. The results from each of the algorithms are presented for the case of a geosynchronous equatorial satellite that makes an evasive maneuver half an orbit before interception. The algorithms are compared and the output validated. The results are presented for two other illustrative cases: maneuvering a quarter of an orbit before a geosynchronous interception and maneuvering two hours before a low-energy direct-ascent interception. A realistic direct-ascent attack is introduced for use as a standard of comparision. Finally, a survey is presented of how required maneuver size varies as a function of required miss distance, maneuver time, and intercept geometry.

In Section VI, the results of the survey are summarized. The thesis concludes with a discussion of the tactics of orbital evasion and with some suggestions for further work.

II. Analytical Development

This section describes the analytical approach. The mathematical model is presented first. Then an algorithm is developed for the case in which the threat is inertially fixed, the time of flight is fixed, and at the end of the flight the satellite must be at a given distance from the threat. Next, a second algorithm is developed incorporating the additional constraint that the trajectory be tangent to a sphere around the threat. A third algorithm allows an extra degree of freedom, in that the time of flight is allowed to vary, although the maneuver time is still held fixed. The final development is to consider a threat that is not fixed but is moving in its own keplerian orbit. It turns out that the moving threat can be used in any of the above three algorithms with little modification.

Mathematical Model of an Orbital Interception

The problem starts with a satellite in a keplerian orbit. There is a threat to the satellite that can be described as a location in space and a distance; the distance might represent the lethal radius of a warhead or the range of a target acquisition radar. At a given time in the future the satellite will be within the sphere defined by the threat's location and the required keep-out distance. A maneuver time is specified. The problem is to

find the smallest maneuver that will result in the satellite being outside the threat sphere at the given time. This is illustrated in Figure 2.1(a): the threat is at point A, and if the satellite does not maneuver it will pierce the threat sphere at B and arrive at C at the time of the threat. Two evasive trajectories are shown based on impulsive maneuvers at D. One trajectory is slower and arrives at E on the threat sphere at the intercept time; the other is faster and passes through the sphere to G by that time.

It can be proved by *reductio ad absurdum* that the optimal trajectory ends exactly on the threat sphere. The dynamics of the problem are those of classical two-body motion, so the orbital state (*i.e.* the position and velocity) of the satellite at the intercept time is a continuous and differentiable function of its state at the maneuver time, although the functional relationship cannot be written explicitly (1:191-203). Therefore infinitesimal changes in the state--in particular, in velocity--at maneuver time will produce infinitesimal changes in state--in particular, in position--at intercept time. If a change in velocity at maneuver time decreases continuously, the position at intercept time will also change continously. If the minimum impulse evasive trajectory did not end at the surface of the threat sphere, it would be possible to decrease the size of the impulse until the trajectory ended at the sphere, producing another evasive trajectory with an

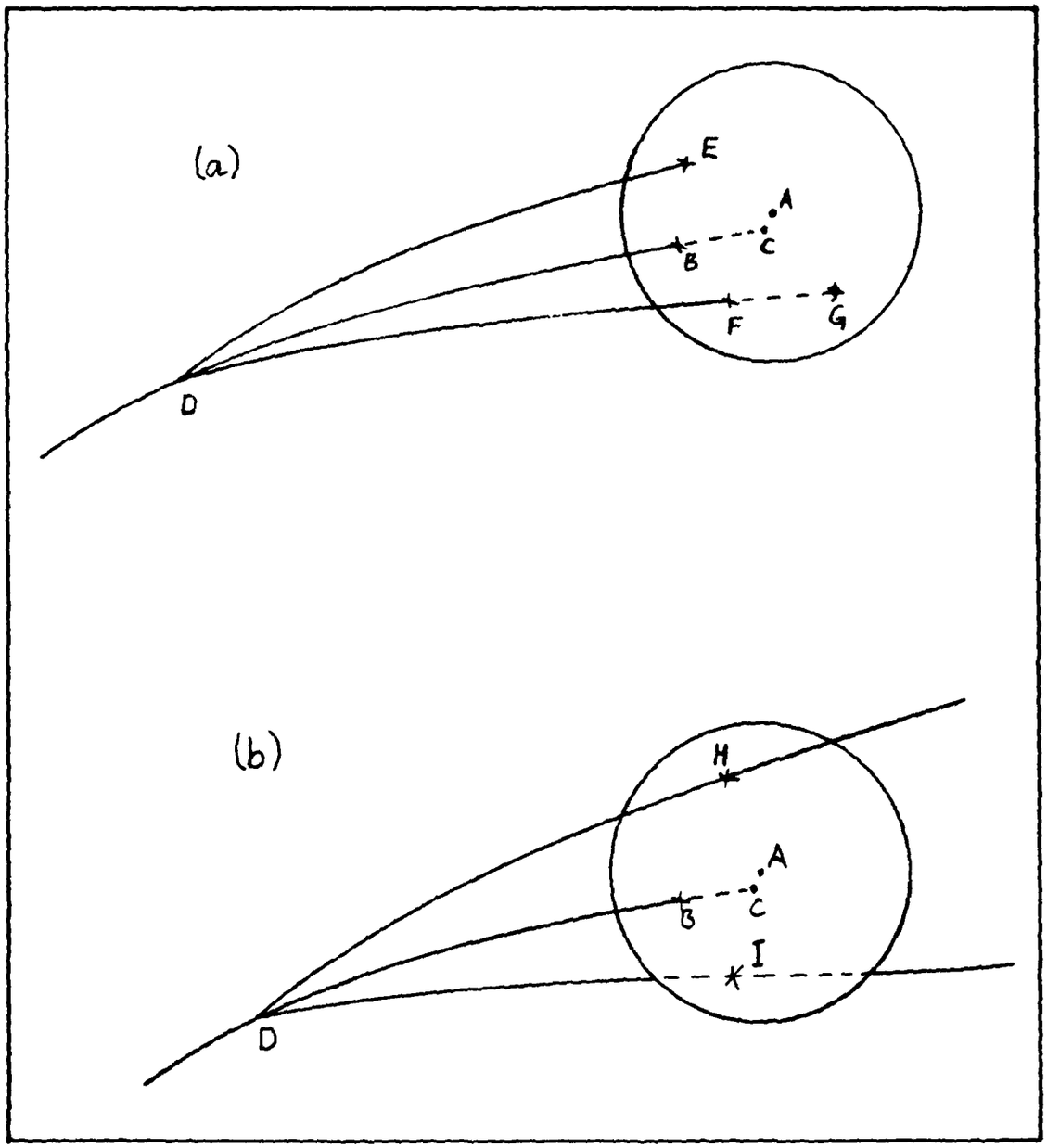

Figure 2.1. Evasive Trajectories:
(a) To the Surface of the Threat Sphere
(b) Tangent to the Threat Sphere

impulse smaller than the minimum. Thus, we need to find the trajectory starting at the maneuver point and ending on the surface of the threat sphere that can be obtained with the smallest total change in velocity at the maneuver time.

Optimal Trajectory to the Threat Sphere

The method used was to develop an iterative algorithm that used the results of one guess at the optimal trajectory to produce a better guess. The line of approach in the next three paragraphs is taken from Wiesel (4).

Let the state vector of the satellite as a function of time be expressed in inertial cartesian coordinates as

$$\underset{\sim}{x}(t) = \left\{ \underset{\sim}{r}(t) \;\; \underset{\sim}{v}(t) \right\}$$
$$= \left\{ x \;\; y \;\; z \;\; \dot{x} \;\; \dot{y} \;\; \dot{z} \right\} \qquad (2.1)$$

When no time is specified, $\underset{\sim}{x}$ will refer to the state vector at intercept time. Let the position of the threat be

$$\underset{\sim}{r}_{th} = \left\{ x_{th} \;\; y_{th} \;\; z_{th} \right\} \qquad (2.2)$$

and let the required miss distance be d. We want to find the optimal trajectory that at intercept time satisfies the constraint

$$|\underset{\sim}{r} - \underset{\sim}{r}_{th}| = d \qquad (2.3)$$

Let us define a function ρ such that

$$\rho = |\underset{\sim}{r} - \underset{\sim}{r}_{th}|$$

$$= \left[(x - x_{th})^2 + (y - y_{th})^2 + (z - z_{th})^2\right]^{1/2} \tag{2.4}$$

(In an attempt to simplify the calculations, ρ was initially defined to be the square of the above expression, but this was found to cause divergence when the initial guess came very close to the threat.) Then the constraint can be expressed as

$$\rho = d \tag{2.5}$$

We can write the 1 x 6 matrix of partial derivatives of ρ with respect to the state as

$$\underset{\sim}{D} = \left[\frac{\partial\rho}{\partial x} \quad \frac{\partial\rho}{\partial y} \quad \frac{\partial\rho}{\partial z} \quad \frac{\partial\rho}{\partial \dot{x}} \quad \frac{\partial\rho}{\partial \dot{y}} \quad \frac{\partial\rho}{\partial \dot{z}}\right]$$

$$= \left[\frac{x - x_{th}}{\rho} \quad \frac{y - y_{th}}{\rho} \quad \frac{z - z_{th}}{\rho} \quad 0 \quad 0 \quad 0\right] \tag{2.6}$$

Infinitesimal changes in ρ are related to infinitesimal changes in $\underset{\sim}{x}$ by

$$\delta\rho = \underset{\sim}{D}\,\delta\underset{\sim}{x} \tag{2.7}$$

Let the state vector at maneuver time be represented by $\underset{\sim}{x}_0 = \{\underset{\sim}{r}_0 \; \underset{\sim}{v}_0\}$. Since the final state is a continuous and differentiable function of the initial state, infinitesimal changes in the final state are related to infinitesimal changes in the initial state by

$$\delta \underset{\sim}{x} = \underset{\sim}{\Phi}\, \delta \underset{\sim}{x}_o \tag{2.8}$$

where

$$\underset{\sim}{\Phi} = \begin{bmatrix} \frac{\partial x}{\partial x_o} & \frac{\partial x}{\partial y_o} & \frac{\partial x}{\partial z_o} & \frac{\partial x}{\partial \dot{x}_o} & \frac{\partial x}{\partial \dot{y}_o} & \frac{\partial x}{\partial \dot{z}_o} \\ \frac{\partial y}{\partial x_o} & \frac{\partial y}{\partial y_o} & \frac{\partial y}{\partial z_o} & \frac{\partial y}{\partial \dot{x}_o} & \frac{\partial y}{\partial \dot{y}_o} & \frac{\partial y}{\partial \dot{z}_o} \\ \frac{\partial z}{\partial x_o} & \frac{\partial z}{\partial y_o} & \frac{\partial z}{\partial z_o} & \frac{\partial z}{\partial \dot{x}_o} & \frac{\partial z}{\partial \dot{y}_o} & \frac{\partial z}{\partial \dot{z}_o} \\ \frac{\partial \dot{x}}{\partial x_o} & \frac{\partial \dot{x}}{\partial y_o} & \frac{\partial \dot{x}}{\partial z_o} & \frac{\partial \dot{x}}{\partial \dot{x}_o} & \frac{\partial \dot{x}}{\partial \dot{y}_o} & \frac{\partial \dot{x}}{\partial \dot{z}_o} \\ \frac{\partial \dot{y}}{\partial x_o} & \frac{\partial \dot{y}}{\partial y_o} & \frac{\partial \dot{y}}{\partial z_o} & \frac{\partial \dot{y}}{\partial \dot{x}_o} & \frac{\partial \dot{y}}{\partial \dot{y}_o} & \frac{\partial \dot{y}}{\partial \dot{z}_o} \\ \frac{\partial \dot{z}}{\partial x_o} & \frac{\partial \dot{z}}{\partial y_o} & \frac{\partial \dot{z}}{\partial z_o} & \frac{\partial \dot{z}}{\partial \dot{x}_o} & \frac{\partial \dot{z}}{\partial \dot{y}_o} & \frac{\partial \dot{z}}{\partial \dot{z}_o} \end{bmatrix} \tag{2.9}$$

However, we can only make changes in velocity at maneuver time, so the left half of $\underset{\sim}{\Phi}$ is of no interest. If $\underset{\sim}{\Psi}$ is the 6 x 3 matrix made up of the right three columns of $\underset{\sim}{\Phi}$, then

$$\delta \underset{\sim}{x} = \underset{\sim}{\Psi}\, \delta \underset{\sim}{v}_o \tag{2.10}$$

Combining Eqs (2.7) and (2.10),

$$\delta \rho = \underset{\sim}{Q}\, \underset{\sim}{\Psi}\, \delta \underset{\sim}{v}_o = \underset{\sim}{E}\, \delta \underset{\sim}{v}_o \tag{2.11}$$

where $\underset{\sim}{E}$ is the 1 x 3 matrix that is the product of $\underset{\sim}{Q}$ and $\underset{\sim}{\Psi}$.

Suppose that we have a trial trajectory that results in a final state $\underset{\sim}{x}$. ρ is evaluated at trajectory end and has the value ρ_t. We would like to find a $\Delta \underset{\sim}{v}_o$ that will

produce a change in ρ of

$$\Delta\rho = d - \rho_t \tag{2.12}$$

$\Delta\rho$ will not be infinitesimal, but using the linear approximation and assuming reasonably small values,

$$\Delta\rho = \underset{\sim}{E}\,\Delta\underset{\sim}{v}_o \tag{2.13}$$

$\Delta\rho$ is known and the components of $\underset{\sim}{E}$ can be calculated; the components of $\Delta\underset{\sim}{v}_o$ are to be found. This is one equation with three unknowns, so it is underdetermined.

There will be an infinite number of components for $\Delta\underset{\sim}{v}_o$ that will satisfy the equation. However, we want the set that will provide the smallest $|\Delta\underset{\sim}{v}_o|$. Thus the problem becomes one of constrained minimization: we need to minimize

$$|\Delta v_o|^2 = \Delta\dot{x}_o^2 + \Delta\dot{y}_o^2 + \Delta\dot{z}_o^2 \tag{2.14}$$

subject to the constraint

$$E_1\Delta\dot{x}_o + E_2\Delta\dot{y}_o + E_3\Delta\dot{z}_o = \Delta\rho \tag{2.15}$$

where the E_i are the elements of $\underset{\sim}{E}$. Since this gives an answer only for the linear approximation, the procedure has to be applied iteratively to converge on the exact solution. The $\Delta\underset{\sim}{v}_o$ determined at each step is applied to $\underset{\sim}{v}_o$ to produce a new trial trajectory. However, the optimization part of each step has as its goal minimizing not the $\Delta\underset{\sim}{v}_o$ for that step, but rather the overall $\Delta\underset{\sim}{v}_o$ relative to the

original trajectory. If $\Delta\underset{\sim}{v}_o$ is the overall trajectory change at the end of the previous iteration, and $\delta\underset{\sim}{v}_o$ is the change to be found in a given step, the quantity to be minimized is (dropping the subscript for brevity)

$$|\Delta\underset{\sim}{v} + \delta\underset{\sim}{v}|^2 = (\Delta\dot{x} + \delta\dot{x})^2 + (\Delta\dot{y} + \delta\dot{y})^2 + (\Delta\dot{z} + \delta\dot{z})^2 \qquad (2.16)$$

Since $\Delta\chi$ is a constant from the previous iteration, this is the same as minimizing

$$\sigma = \delta x^2 + \delta y^2 + \delta z^2 + 2\Delta\dot{x}\delta\dot{x} + 2\Delta\dot{y}\delta\dot{y} + 2\Delta\dot{z}\delta\dot{z} \qquad (2.17)$$

We can use the constraint (Eq [2.15]) to eliminate one variable from the objective function σ. If we eliminate $\delta\dot{z}$, then

$$\sigma = \alpha\delta\dot{x}^2 + \beta\delta\dot{y}^2 + \gamma\delta\dot{x} + \varepsilon\delta\dot{y} + \zeta\delta\dot{x}\delta\dot{y} + \eta \qquad (2.18)$$

where

$$\alpha = 1 + \frac{E_1^2}{E_3^2} \qquad (2.19)$$

$$\beta = 1 + \frac{E_2^2}{E_3^2} \qquad (2.20)$$

$$\gamma = 2\left[\Delta\dot{x} - \frac{E_1}{E_3}\left(\frac{\Delta\varrho}{E_3} + \Delta\dot{z}\right)\right] \qquad (2.21)$$

$$\varepsilon = 2\left[\Delta\dot{y} - \frac{E_2}{E_3}\left(\frac{\Delta\varrho}{E_3} + \Delta\dot{z}\right)\right] \qquad (2.22)$$

$$\zeta = \frac{2E_1E_2}{E_3^2} \qquad (2.23)$$

$$\eta = \frac{\Delta\varrho^2}{E_3^2} + 2\Delta\dot{z}\frac{\Delta\varrho}{E_3} \qquad (2.24)$$

Note that the objective function is quadratic and has strictly postive coefficients on $\delta\dot{x}^2$ and $\delta\dot{y}^2$. The cross term could be negative, but it would dominate the function only when both $\delta\dot{x}$ and $\delta\dot{y}$ were large in magnitude, and then

$$\sigma \approx \left(1+\frac{E_1^2}{E_3^2}\right)\delta\dot{x}^2 + \left(1+\frac{E_2^2}{E_3^2}\right)\delta\dot{y}^2 + \frac{2E_1E_2}{E_3^2}\delta\dot{x}\,\delta\dot{y}$$

$$\approx \left(1+\frac{E_1^2}{E_3^2}+1+\frac{E_2^2}{E_3^2} \pm \frac{2E_1E_2}{E_3^2}\right)\delta\dot{x}^2$$

$$\approx \left[2+\frac{(E_1 \pm E_2)^2}{E_3^2}\right]\delta\dot{x}^2 \qquad (2.25)$$

making σ large and positive. Therefore the function represents a sheet in the $\delta\dot{x}$-$\delta\dot{y}$ plane concave upwards, and it has a unique minimum.

An extremum will occur when

$$\frac{\partial\sigma}{\partial\delta\dot{x}} = 2\alpha\,\delta\dot{x} + \gamma + \zeta\,\delta\dot{y} = 0 \qquad (2.26)$$

and

$$\frac{\partial\sigma}{\partial\delta\dot{y}} = 2\beta\,\delta\dot{y} + \varepsilon + \zeta\,\delta\dot{x} = 0 \qquad (2.27)$$

With two linear equations and two unknowns, we can solve for $\delta\dot{x}$ and $\delta\dot{y}$:

$$\delta\dot{x} = \frac{\varepsilon\zeta - 2\beta\gamma}{4\alpha\beta - \zeta^2} \tag{2.28}$$

$$\delta\dot{y} = \frac{-\varepsilon - \zeta\,\delta\dot{x}}{2\beta} \tag{2.29}$$

$\delta\dot{z}$ can then be obtained from Eq (2.15), and $\delta\underset{\sim}{v}_o$ is entirely determined. It can then be applied to $\underset{\sim}{v}_o + \Delta\underset{\sim}{v}_o$ to produce a new trial trajectory, which should have a smaller value for $\Delta\rho$ at the intercept.

Note that we could chance upon a trial trajectory that produced a zero value for $\Delta\rho$ but still was not optimal. It is necessary to continue to iterate until $\delta\underset{\sim}{v}_o$ goes to zero as well as $\Delta\rho$. This will guarantee that there are no nearby trajectories that also give the desired final conditions but at a smaller maneuver cost.

Optimal Trajectory Tangent to the Threat Sphere

The trajectory produced by the above algorithm will put the satellite at the surface of the threat sphere at the time of interception, but the trajectory is very likely to pass through the sphere either before or after that moment (Figure 2.1[a]). This may be acceptable if the threat is known to be an instantaneous one, such as a high-velocity interceptor that will cross the satellite's orbit at a known time. In other cases, it may be desirable that the satellite never enter the threat sphere at all. In such a situation we need the optimal trajectory that

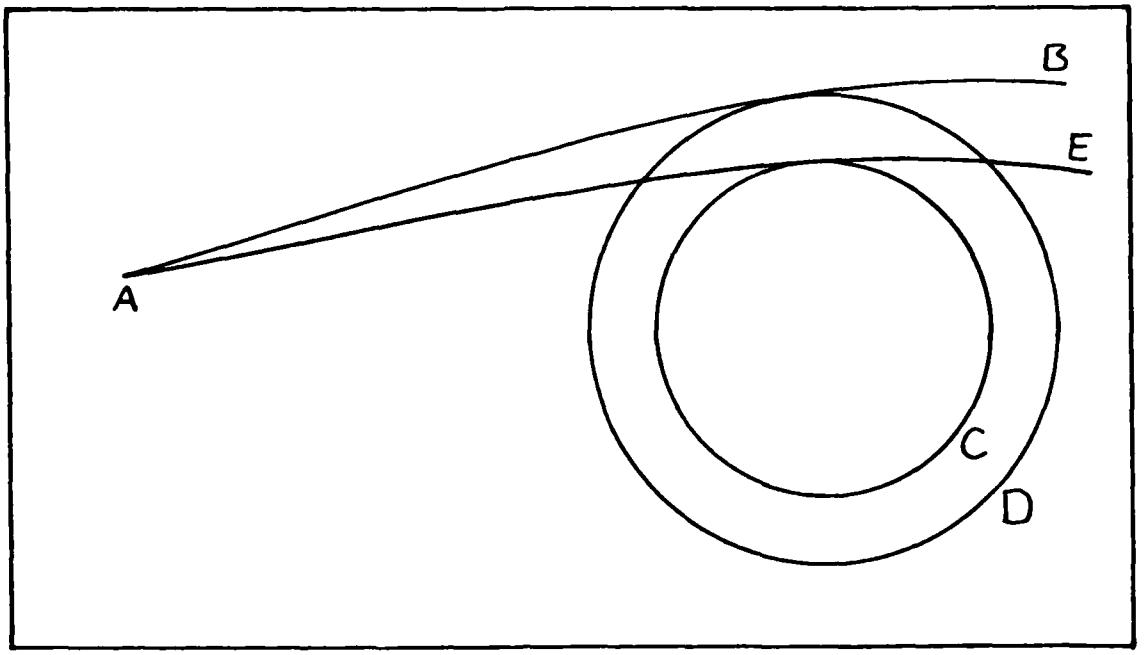

Figure 2.2. Tangent Trajectories to Concentric Spheres

touches the threat sphere but does not pierce it. This is shown in Figure 2.1(b), where the evasion trajectories DH and DI are tangent to the sphere on nearly opposite sides.

If the trajectory must never enter the threat sphere, it is not as simple to prove rigorously that the optimal trajectory touches the sphere as it was when the orbit could pierce the sphere. However, a practical proof is still possible. In Figure 2.2, suppose that AB is the optimal evasion trajectory for threat sphere C, which it does not touch. A larger sphere D is tangent to AB. AB must be the optimal evasion trajectory for D, since any better trajectory would also be an evasive trajectory for C. If AE is the best possible trajectory tangent to C, then AE by supposition must be less optimal (i.e. require a

larger impulse at A) than AB. Therefore the best trajectory tangent to the larger sphere requires a smaller impulse than the best trajectory tangent to the smaller sphere. This is contrary to the results in Section V (Figure 5.5): it was found that the impulse for the best tangent trajectory grew linearly with sphere radius. Therefore the optimal evasive trajectory should be tangent to the threat sphere.

To find this trajectory, an additional constraint must be imposed on the state vector at intercept time.

Let us define a function ξ such that

$$\begin{aligned} \xi &= (\underset{\sim}{r} - \underset{\sim}{r}_m) \cdot \underset{\sim}{v} \\ &= (x - x_m)\dot{x} + (y - y_m)\dot{y} + (z - z_m)\dot{z} \end{aligned} \tag{2.30}$$

Then the constraint that the satellite's velocity be tangent to the threat sphere is expressed as

$$\xi = 0 \tag{2.31}$$

at the intercept time. With this additional constraint imposed, it is necessary to redefine $\underset{\sim}{D}$ as

$$\underset{\sim}{D} = \begin{bmatrix} \frac{\partial \rho}{\partial x} & \frac{\partial \rho}{\partial y} & \frac{\partial \rho}{\partial z} & \frac{\partial \rho}{\partial \dot{x}} & \frac{\partial \rho}{\partial \dot{y}} & \frac{\partial \rho}{\partial \dot{z}} \\ \frac{\partial \xi}{\partial x} & \frac{\partial \xi}{\partial y} & \frac{\partial \xi}{\partial z} & \frac{\partial \xi}{\partial \dot{x}} & \frac{\partial \xi}{\partial \dot{y}} & \frac{\partial \xi}{\partial \dot{z}} \end{bmatrix}$$

$$= \begin{bmatrix} \frac{x-x_{th}}{\rho} & \frac{y-y_{th}}{\rho} & \frac{z-z_{th}}{\rho} & 0 & 0 & 0 \\ \dot{x} & \dot{y} & \dot{z} & x-x_{th} & y-y_{th} & z-z_{th} \end{bmatrix} \tag{2.32}$$

(analogous to Eq [2.6]). Then

$$\begin{bmatrix} \delta\rho \\ \delta\xi \end{bmatrix} = \underset{\sim}{D}\,\delta\underset{\sim}{x} = \underset{\sim}{D}\,\underset{\sim}{\Psi}\,\delta\underset{\sim}{v}_o = \underset{\sim}{E}\,\delta\underset{\sim}{v}_o \tag{2.33}$$

where $\underset{\sim}{E}$ is here a 2 x 3 matrix.

Given a trial trajectory, we can calculate ρ and ξ at intercept time. $\Delta\rho$, the desired change in ρ, is still given by Eq (2.12), and

$$\Delta\xi = -\xi \tag{2.34}$$

In the linear approximation,

$$\begin{bmatrix} \Delta\rho \\ \Delta\xi \end{bmatrix} = \underset{\sim}{E}\,\delta\underset{\sim}{v}_o \tag{2.35}$$

This is a system of two equations with three unknowns.

The objective function θ is still as given by Eq (2.17), but now two of the variables can be eliminated because we have two constraints in Eq (2.35). If $\delta\dot{y}$ and $\delta\dot{z}$ are eliminated, then

$$\theta = \zeta\,\delta\dot{x}^2 + \eta\,\delta\dot{x} + \theta \tag{2.36}$$

where

$$\alpha = \frac{E_{33}E_{11} - E_{21}E_{13}}{E_{13}E_{22} - E_{23}E_{12}} \tag{2.37}$$

$$\beta = \frac{E_{13}\Delta\xi - E_{23}\Delta\rho}{E_{13}E_{22} - E_{23}E_{12}} \tag{2.38}$$

$$\gamma = \frac{E_{22}E_{11} - E_{21}E_{12}}{E_{12}E_{23} - E_{22}E_{13}} \tag{2.39}$$

$$\varepsilon = \frac{E_{12}\Delta\xi - E_{22}\Delta\rho}{E_{12}E_{23} - E_{22}E_{13}} \tag{2.40}$$

$$\zeta = 1 + \alpha^2 + \gamma^2 \tag{2.41}$$

$$\eta = 2\left[\Delta\dot{x} + \alpha\left(\beta + \Delta\dot{y}\right) + \gamma\left(\varepsilon + \Delta\dot{z}\right)\right] \tag{2.42}$$

$$\theta = \beta^2 + 2\beta\Delta\dot{y} + \varepsilon^2 + 2\varepsilon\Delta\dot{z} \tag{2.43}$$

and the E_{ij} are the elements of $\underset{\sim}{E}$ (α through η have been redefined from their use in Eqs [2.19] through [2.24]). Note that θ is again quadratic with a strictly positive second-order coefficient, so it has a unique minimum. Setting its derivative equal to zero,

$$\delta\dot{x} = -\frac{\eta}{2\zeta} \tag{2.44}$$

The other components of $\delta\underset{\sim}{v}_o$ are

$$\delta\dot{y} = \alpha\,\delta\dot{x} + \beta \tag{2.45}$$

$$\delta\dot{z} = \gamma\,\delta\dot{x} + \varepsilon \tag{2.46}$$

Allowing Time of Flight to Vary

The above algorithm restricts the time of flight between the maneuver and the tangency point: it must be the same as the original time between the maneuver point and the interception. This is probably not a realistic restriction. If anything, it would be advantageous for the time of closest approach to be different from the expected intercept time. The next step in the analysis is to include time of flight as a variable. The maneuver time will be held fixed, but the time when the satellite is at the tangency point will change.

Time of flight can be considered as a another variable besides $\delta \underset{\sim}{v}_o$ that determines a new $\underset{\sim}{x}$. Eq (2.10) must be rewritten as

$$\delta \underset{\sim}{x} = \underset{\sim}{\Psi} \left\{ \delta \dot{x}_o \quad \delta \dot{y}_o \quad \delta \dot{z}_o \quad \delta t \right\} \tag{2.47}$$

where $\underset{\sim}{\Psi}$ has been augmented to a 6 x 4 matrix, the rightmost column of which relates infinitesimal changes in time to infinitesimal changes in final state. In other words, this column contains the partial derivatives of the state with respect to time, which are just the velocity and acceleration of the satellite. The velocity is part of the state vector and the acceleration is the acceleration of gravity, so the last column of $\underset{\sim}{\Psi}$ is

$$\left\{ \dot{x} \quad \dot{y} \quad \dot{z} \quad -\frac{\mu x}{r^3} \quad -\frac{\mu y}{r^3} \quad -\frac{\mu z}{r^3} \right\} \tag{2.48}$$

where μ is the gravitational parameter of the Earth.

Eq (2.33) still holds, but $\underset{\sim}{E}$ is now a 2 x 4 matrix. The objective function is still as in Eq (2.17), but the constraints are represented by

$$\begin{bmatrix} \Delta\varrho \\ \Delta\xi \end{bmatrix} = \underset{\sim}{E} \left\{ \delta\dot{x} \;\; \delta\dot{y} \;\; \delta\dot{z} \;\; \delta t \right\} \tag{2.49}$$

a system of two equations with four unknowns. Note that one of the unknowns, δt, does not occur in the objective function. One of the constraint equations must be used to eliminate δt from the other, which then can be used to eliminate one variable from θ. If this is done, we obtain

$$\theta = \varepsilon\delta\dot{x}^2 + \zeta\delta\dot{y}^2 + \eta\delta\dot{x}\delta\dot{y} + \theta\delta\dot{x} + \iota\delta\dot{y} + \kappa \tag{2.50}$$

where here the coefficients are defined by the following:

$$\alpha = \frac{E_{14}E_{21} - E_{24}E_{11}}{E_{24}E_{13} - E_{14}E_{23}} \tag{2.51}$$

$$\beta = \frac{E_{14}E_{22} - E_{24}E_{12}}{E_{24}E_{13} - E_{14}E_{23}} \tag{2.52}$$

$$\gamma = \frac{E_{24}\Delta\varrho - E_{14}\Delta\xi}{E_{24}E_{13} - E_{14}E_{23}} \tag{2.53}$$

$$\varepsilon = 1 + \alpha^2 \tag{2.54}$$

$$\zeta = 1 + \beta^2 \tag{2.55}$$

$$\eta = 2\alpha\beta \tag{2.56}$$

$$\theta = 2\left[\alpha(\gamma + \Delta\dot{z}) + \Delta\dot{x}\right] \tag{2.57}$$

$$\iota = 2\left[\beta(\gamma + \Delta\dot{z}) + \Delta\dot{y}\right] \tag{2.58}$$

$$\kappa = \gamma^2 + 2\Delta\dot{z}\gamma \tag{2.59}$$

Again θ has a unique minimum, and

$$\delta\dot{x} = \frac{\eta\iota - 2\zeta\theta}{4\varepsilon\zeta - \eta^2} \tag{2.60}$$

$$\delta\dot{y} = -\frac{\eta\delta\dot{x} + \iota}{2\zeta} \tag{2.61}$$

$$\delta\dot{z} = \alpha\delta\dot{x} + \beta\delta\dot{y} + \gamma \tag{2.62}$$

$$\delta t = \frac{1}{E_{14}}\left(\Delta\xi - E_{21}\delta\dot{x} - E_{22}\delta\dot{y} - E_{23}\delta\dot{z}\right) \tag{2.63}$$

Note that it has been assumed that the tangency constraint has been imposed. If it is not, the avoidance problem becomes trivial when time of flight is allowed to vary. By choosing the trajectory end time as the moment when the satellite enters the threat sphere, the only constraint (on radial distance) is satisfied without any maneuver at all.

Only the end time of the trajectory was allowed to vary, but the maneuver time can also be made a variable. This approach was not explored because of an expectation that it would always be better to maneuver earlier. As will be discussed in Section V, this turned out to be generally but not quite universally true.

The Moving Attacker

Up to this point the threat has been considered as fixed in inertial space. In a real attack, the interceptor would be a missile or satellite moving in an orbit of its own. If the interceptor carried a homing device of a certain range or an explosive warhead whose time of detonation was unknown, the evasive trajectory would be required never to take the satellite closer than a fixed distance to the moving threat. We want the minimum impulse trajectory such that at the time of closest approach to the threat, the distance between the two spacecraft is equal to the required keep-out range. The satellite's trajectory must now be tangent to the threat sphere not in the geocentric frame of reference but rather in the moving frame of reference of the sphere itself. Thus, if the state vector of the attacker at intercept time is $\underset{\sim}{x}_{th}$, we must consider the state vector of the satellite with respect to the threat:

$$\underset{\sim}{x}_{rel} = \underset{\sim}{x} - \underset{\sim}{x}_{th} \tag{2.64}$$

We have used the error functions ρ and ξ (defined by Eqs [2.4] and [2.30]) to represent the constraints on the trajectory. The distance constraint is not affected by the motion of the attacker, so the ρ constraint is unchanged. The ξ constraint must be rewritten as

$$\xi = \underset{\sim}{r}_{rel} \cdot \underset{\sim}{v}_{rel} = (\underset{\sim}{r} - \underset{\sim}{r}_{th}) \cdot (\underset{\sim}{v} - \underset{\sim}{v}_{th})$$

$$= (x - x_{th})(\dot{x} - \dot{x}_{th}) + (y - y_{th})(\dot{y} - \dot{y}_{th}) + (z - z_{th})(\dot{z} - \dot{z}_{th}) \tag{2.65}$$

$\underset{\sim}{D}$ should now be calculated as the the matrix of partials of the error functions with respect to the relative state:

$$\underset{\sim}{D} = \begin{bmatrix} \frac{x - x_{th}}{\rho} & \frac{y - y_{th}}{\rho} & \frac{z - z_{th}}{\rho} & 0 & 0 & 0 \\ \dot{x} - \dot{x}_{th} & \dot{y} - \dot{y}_{th} & \dot{z} - \dot{z}_{th} & x - x_{th} & y - y_{th} & z - z_{th} \end{bmatrix} \tag{2.66}$$

where the only difference from Eq (2.32) is the subtraction of threat velocity from the first three terms of the second row. Likewise, $\underset{\sim}{\Psi}$ should now be considered the matrix of partials of the relative state with respect to the independent variables $\delta\underset{\sim}{v}_o$ and δt. Since the absolute state of the threat is independent of $\delta\underset{\sim}{v}_o$, the left three columns of $\underset{\sim}{\Psi}$ are the same as before. However, the state of the threat does change with time, so the elements of the rightmost column of $\underset{\sim}{\Psi}$ become

$$\left\{ \dot{x} - \dot{x}_{th} \;\; \dot{y} - \dot{y}_{th} \;\; \dot{z} - \dot{z}_{th} \;\; -\frac{\mu x}{r^3} + \frac{\mu x_{th}}{r_{th}^3} \;\; -\frac{\mu y}{r^3} + \frac{\mu y_{th}}{r_{th}^3} \;\; -\frac{\mu z}{r^3} + \frac{\mu z_{th}}{r_{th}^3} \right\} \tag{2.67}$$

(compare with Eq [2.48]).

With $\underset{\sim}{D}$ and $\underset{\sim}{\Psi}$ redefined in this way, any of the three algorithms already described can be used to calculate opti-

mal corrections to $\underset{\sim}{v}_0$ and converge on the best evasive trajectory. Of course, in the first algorithm, in which the time of flight is fixed and no tangency constraint is imposed, there is no point to using this modification, since the motion of the threat is irrelevant to the problem.

III. Computer Implementation

This section describes how the mathematical algorithms were translated into a working computer program. After a general description of the program, the method of generating the matrix $\underset{\sim}{\Phi}$ is presented. The criteria used to establish convergence are described and the method of dealing with multiple solutions are given. The final subsection shows how it was proven that the time of closest approach found by the algorithms imposing the tangency constraint was in fact the global closest approach to the threat.

General Description

The program was written in FORTRAN 77 and run on the VAX 11/785 Scientific Support Computer (SSC) under the UNIX operating system at the School of Engineering of the Air Force Institute of Technology. The program contains about 1900 lines of code in 22 separately compiled subroutines. The program generally conforms to good programming practice but does not have extensive comments. Orbit calculations are all done in double precision using the universal variable formulation found in Bate, Mueller, and White (1:191-210). The program takes the satellite and threat state vectors from an input file, along with the maneuver and intercept times and the keep-out distance. If the

threat velocity vector is null, the threat is treated as inertially fixed. The same program runs all three algorithms. The orbital calculations are the same for all three, and logical input variables control which set of equations is used to calculate $\delta \underset{\sim}{v}_0$. Another input variable causes the printing of intermediate results for debugging and verification. Some checks are done on the reasonability of the input. The limits of convergence and the maximum number of iterations were coded into the program and were the same for each run, but they can be changed in the code fairly easily. In general the program contains little protection against numerical problems and singularities--such protection was put in only when a problem occurred.

Generating the Phi Matrix

The matrix $\underset{\sim}{\Phi}$ is the 6 x 6 matrix of the partial derivatives of components of the end state with respect to components of the beginning state, as shown in Eq (2.9). The algorithms require that the right three columns of $\underset{\sim}{\Phi}$ be calculated for each trial trajectory, since they form the left three columns of $\underset{\sim}{\Psi}$. The matrix $\underset{\sim}{\Phi}$ can be derived in several ways, including integrating the equations of variation along the trajectory (4). In the two-body problem it can be calculated exactly, and this is what was done. The method used was to express the end state in terms of the f and g functions described in Bate, Mueller, and White

(1:198), and then differentiate it with liberal use of the chain rule.

The end state can be written as

$$\underset{\sim}{r} = f\underset{\sim}{r_0} + g\underset{\sim}{v_0} \tag{3.1}$$

$$\underset{\sim}{v} = \dot{f}\underset{\sim}{r_0} + \dot{g}\underset{\sim}{v_0} \tag{3.2}$$

(1:198). With some notation conventions, $\underset{\sim}{\Phi}$ can be compactly represented in terms of its four 3 x 3 submatrices. Let us take a partial with respect to a vector to mean the vector of partials with respect to the vector elements, so that

$$\frac{\partial f}{\partial \underset{\sim}{r_0}} = \left\{ \frac{\partial f}{\partial x_0} \quad \frac{\partial f}{\partial y_0} \quad \frac{\partial f}{\partial z_0} \right\} \tag{3.3}$$

$$\frac{\partial \dot{g}}{\partial \underset{\sim}{v_0}} = \left\{ \frac{\partial \dot{g}}{\partial \dot{x}_0} \quad \frac{\partial \dot{g}}{\partial \dot{y}_0} \quad \frac{\partial \dot{g}}{\partial \dot{z}_0} \right\} \tag{3.4}$$

and so on. Also, for any two vectors $\underset{\sim}{a}$ and $\underset{\sim}{b}$, let their vector matrix product be defined by

$$\underset{\sim}{a}\,\underset{\sim}{b} = \begin{bmatrix} a_x b_x & a_x b_y & a_x b_z \\ a_y b_x & a_y b_y & a_y b_z \\ a_z b_x & a_z b_y & a_z b_z \end{bmatrix} \tag{3.5}$$

and let $\underset{\sim}{I}$ represent the identity matrix. Then

$$\underset{\sim}{\Phi} = \begin{bmatrix} f\underset{\sim}{I} + \underset{\sim}{r_0}\frac{df}{d\underset{\sim}{r_0}} + \underset{\sim}{v_0}\frac{dg}{d\underset{\sim}{r_0}} & g\underset{\sim}{I} + \underset{\sim}{r_0}\frac{df}{d\underset{\sim}{v_0}} + \underset{\sim}{v_0}\frac{dg}{d\underset{\sim}{v_0}} \\ \dot{f}\underset{\sim}{I} + \underset{\sim}{r_0}\frac{d\dot{f}}{d\underset{\sim}{r_0}} + \underset{\sim}{v_0}\frac{d\dot{g}}{d\underset{\sim}{r_0}} & \dot{g}\underset{\sim}{I} + \underset{\sim}{r_0}\frac{d\dot{f}}{d\underset{\sim}{v_0}} + \underset{\sim}{v_0}\frac{d\dot{g}}{d\underset{\sim}{v_0}} \end{bmatrix} \tag{3.6}$$

The f, g, $\dot{f}$, and $\dot{g}$ functions are given by

$$f = 1 - \frac{x^2}{r_0} C \tag{3.7}$$

$$g = t - \frac{x^3}{\mu^{1/2}} S \tag{3.8}$$

$$\dot{f} = -\frac{(\mu a)^{1/2}}{r_0 r} \sin(\gamma^{1/2}) \tag{3.9}$$

$$\dot{g} = 1 - \frac{x^2}{r} C \tag{3.10}$$

(1:201-202). Here r_0 is the magnitude of the position vector at trajectory start, r is its magnitude at trajectory end, t is the time elapsed on the trajectory, μ is the Earth's gravitational parameter, a is the semimajor axis of the trajectory orbit, and the other variables can be calculated from

$$C = \frac{1 - \cos(\gamma^{1/2})}{\gamma} \tag{3.11}$$

$$S = \frac{\gamma^{1/2} - \sin(\gamma^{1/2})}{\gamma^{3/2}} \tag{3.12}$$

$$\gamma = \frac{x^2}{a} \tag{3.13}$$

and the universal variable x, which cannot be given explicitly but can be found from

$$\mu^{1/2} t = \mathcal{x}^3 S + \frac{r_0 \cdot v_0}{\mu^{1/2}} \mathcal{x}^2 C + r_0 a^{1/2} \sin(\mathcal{y}^{1/2}) \tag{3.14}$$

(1:195-196). $\mathcal{x}$ and $\mathcal{y}$ are written in script to distinguish them from the x- and z-coordinates.

The differentiation can begin by evaluating the following:

$$\underset{\sim}{R}_0 = \frac{\partial r_0}{\partial \underset{\sim}{x}_0} = \left\{ \frac{x_0}{r} \quad \frac{y_0}{r} \quad \frac{z_0}{r} \quad 0 \quad 0 \quad 0 \right\} \tag{3.15}$$

$$\underset{\sim}{V}_0 = \frac{\partial v_0}{\partial \underset{\sim}{x}_0} = \left\{ 0 \quad 0 \quad 0 \quad \frac{\dot{x}_0}{v_0} \quad \frac{\dot{y}_0}{v_0} \quad \frac{\dot{z}_0}{v_0} \right\} \tag{3.16}$$

$$\frac{\partial a}{\partial \underset{\sim}{x}_0} = \frac{\partial}{\partial x_0} \left[\frac{1}{\frac{2}{r_0} - \frac{v_0^2}{\mu}} \right]$$

$$= 2a^2 \underset{\sim}{R}_3 \tag{3.17}$$

where

$$\underset{\sim}{R}_3 = \left\{ \frac{x_0}{r_0^3} \quad \frac{y_0}{r_0^3} \quad \frac{z_0}{r_0^3} \quad \frac{\dot{x}_0}{\mu} \quad \frac{\dot{y}_0}{\mu} \quad \frac{\dot{z}_0}{\mu} \right\} \tag{3.18}$$

Using Eq (3.17) one finds that

$$\frac{\partial \mathcal{x}}{\partial \underset{\sim}{x}_0} = \frac{2\mathcal{x}}{a} \frac{\partial \mathcal{x}}{\partial \underset{\sim}{x}_0} - 2\mathcal{x}^2 \underset{\sim}{R}_3 \tag{3.19}$$

In addition,

$$\frac{dC}{d\mathcal{y}} = \frac{1 - 2C - S\mathcal{y}}{2\mathcal{y}} \tag{3.20}$$

$$\frac{dS}{d\gamma} = \frac{C-3S}{2\gamma} \tag{3.21}$$

(1:210). Using these, one can perform the differentiation of f and g to to find that

$$\frac{\partial f}{\partial \underset{\sim}{x}_0} = -\frac{a^{1/2}}{r_0}\sin(\gamma^{1/2})\frac{\partial \alpha}{\partial \underset{\sim}{x}_0} + \frac{a\alpha^2}{r_0}(1-2C-S\gamma)\underset{\sim}{R}_3 + \frac{\alpha^2}{r_0^2}C\,\underset{\sim}{R}_0 \tag{3.22}$$

$$\frac{\partial g}{\partial \underset{\sim}{x}_0} = -\frac{\alpha^2}{\mu^{1/2}}C\frac{\partial \alpha}{\partial \underset{\sim}{x}_0} + \frac{a\alpha^3}{\mu^{1/2}}(C-3S)\underset{\sim}{R}_3 \tag{3.23}$$

where everything is known except $\frac{\partial \alpha}{\partial \underset{\sim}{x}_0}$.

Before finding the partial derivatives of $\dot{f}$ and $\dot{g}$, it is convenient to evaluate the following:

$$\underset{\sim}{P} = \frac{\partial(\underset{\sim}{r}_0\cdot\underset{\sim}{v}_0)}{\partial \underset{\sim}{x}_0} = \left\{ \dot{x}_0 \;\; \dot{y}_0 \;\; \dot{z}_0 \;\; x_0 \;\; y_0 \;\; z_0 \right\} \tag{3.24}$$

$$\underset{\sim}{R} = \frac{\partial r}{\partial \underset{\sim}{x}_0} = \frac{1}{r}\left[\underset{\sim}{F} + fg\,\underset{\sim}{P} + (r_0^2 f + g\,\underset{\sim}{r}_0\cdot\underset{\sim}{v}_0)\frac{\partial f}{\partial \underset{\sim}{x}_0} + (v_0^2 g + f\,\underset{\sim}{r}_0\cdot\underset{\sim}{v}_0)\frac{\partial g}{\partial \underset{\sim}{x}_0}\right] \tag{3.25}$$

where

$$\underset{\sim}{F} = \left\{ f^2x_0 \;\; f^2y_0 \;\; f^2z_0 \;\; g^2\dot{x}_0 \;\; g^2\dot{y}_0 \;\; g^2\dot{z}_0 \right\} \tag{3.26}$$

Then

$$\frac{\partial \dot{f}}{\partial \underset{\sim}{x}_0} = \frac{\mu^{1/2}}{r_0 r}\left[\frac{a^{1/2}\sin(\eta^{1/2})}{r_0}\underset{\sim}{R}_0 + \frac{a^{1/2}\sin(\eta^{1/2})}{r}\underset{\sim}{R} - \cos(\eta^{1/2})\frac{\partial \chi}{\partial \underset{\sim}{x}_0} + \chi^3 (S-C)\underset{\sim}{R}_3\right] \qquad (3.27)$$

$$\frac{\partial \dot{g}}{\partial \underset{\sim}{x}_0} = \frac{a\chi^2}{r}(1-2C-S\eta)\underset{\sim}{R}_3 - \frac{a^{1/2}}{r}\sin(\eta^{1/2})\frac{\partial \chi}{\partial \underset{\sim}{x}_0} + \frac{\chi^2}{r^2}C\underset{\sim}{R} \qquad (3.28)$$

Again everything is known except $\frac{\partial \chi}{\partial x_0}$, which is now the only element needed to find $\underset{\sim}{\Phi}$.

This final partial can be evaluated from Eq (3.14). Time is held constant, since we are interested in how the universal variable χ changes when small changes are made in the initial state without changing the time of flight. The result is

$$\frac{\partial \chi}{\partial \underset{\sim}{x}_0} = \frac{\left\{\chi^3\left[(C-S)(a-r_0)-2aS\right]+\frac{\underset{\sim}{r}_0\cdot\underset{\sim}{v}_0}{\mu^{1/2}}a\chi^2(1-2C-S\eta)\right\}\underset{\sim}{R}_3 - \frac{\chi^2}{\mu^{1/2}}C\underset{\sim}{P} - a^{1/2}\sin(\eta^{1/2})\underset{\sim}{R}_0}{\chi^2 C + r_0\cos(\eta^{1/2}) + \frac{\underset{\sim}{r}_0\cdot\underset{\sim}{v}_0}{\mu^{1/2}}a^{1/2}\sin(\eta^{1/2})} \qquad (3.28)$$

When converging on an optimum orbit, $\underset{\sim}{\Phi}$ hardly changes at all after the first couple of iterations (4). Computer run time could probably be reduced somewhat by not recalculating the matrix at every step. On the other hand, the burden of calculating it is not excessive, since most of

the values needed are available as by-products of finding the end state. The program as written recalculates $\underset{\sim}{\Phi}$ at every iteration.

Convergence Criteria

In an iterative algorithm, criteria must be selected for deciding when one is close enough to the exact answer to stop calculating. For this program, a miss distance accuracy of 10 meters was selected as at or beyond the limit of practical orbital determination and as negligibly small compared to the threat sphere radii used (hundreds of kilometers). A closing rate accuracy of 0.1 meters per second was selected as being zero for all practical purposes. The values used to determine convergence in the program were based on these numbers.

Different criteria were established for $\Delta\rho$, $\Delta\xi$, δt, and $\delta\underset{\sim}{v}_o$. Since the error function ρ is the required miss distance, $\Delta\rho$ was considered converged when its magnitude became less than 10 meters. Since ξ is the dot product of the relative position and velocity vectors, the closing velocity at the threat sphere is given by $-\xi/d$, where d is the sphere radius. Therefore the convergence limit for $\Delta\xi$ was $0.1d$ meters per second. The convergence criterion for δt was set at 0.0009 seconds so that even at the highest possible elliptical orbit velocities the final position would be accurate within 10 meters. These were all values defined at the end of the trajectory and their limits were

straightforward; the problem of convergence limits on δv_0 was somewhat subtler. In the infinitesimal limit, changes in initial velocity are related to changes in final position by the upper right 3 x 3 submatrix of Φ. The highest values observed there were on the order of 100,000. This required that the maneuver velocity be accurate within 0.0001 meters per second, which was the limit initially used. In any iterative procedure, however, iterations can be stopped after corrections have become smaller than the ultimate desired accuracy only when convergence is rapid enough that most of the remaining distance to the true solution is covered at each step. If the corrections at each step are only slightly smaller than the previous ones, then the procedure can be converging and the individual corrections can be negligibly small when there is still a significant distance to go to the true answer. As will be described in the Section IV, this problem was encountered and required even stricter limits on velocity corrections.

Finding Multiple Solutions

The convergence of the algorithm on a particular solution proves only that that solution is locally optimal, not that it is the best of all possible maneuvers. Also, there is no guarantee that the algorithm will converge from any particular starting guess. To ensure finding all the locally optimal solutions, the algorithm was run nine times for each problem with nine different initial guesses. The

first initial guess was the original orbit; the other eight were positive and negative changes in each of the four decision variables (velocity and time) large enough to move the end position by a distance equal to the threat radius. It was found that usually at least seven of the nine converged, and that there were almost always exactly two locally optimal solutions. The only exceptions were when the original interception came no closer to the target than about one third of the threat radius; in these cases only one solution was found. Whenever this happened, the program searched for a second optimal solution using another twelve initial guesses, which varied the decision variables in pairs. No second solution was ever found from the extra twelve runs except when for some reason most of the initial nine attempts had not converged. No third solution was ever found, although nine attempts were always made. The writer conjectures that two locally optimal solutions are the largest number that ever occur.

Ruling Out a Second Close Approach

Since the algorithm examines the evasive trajectories only at the maneuver time and at the time of closest approach (TCA), one cannot *a priori* rule out the possibility that there is another closer approach either before or after the TCA. To eliminate this possibility, the relative position of the satellite was calculated ten seconds before and after the TCA for each locally optimal solution. If

the satellite was still outside the threat sphere, a subsequent time (or a previous time, for the check before TCA) was calculated at which to evaluate the satellite's relative position again. This subsequent time was the time at which the satellite would be at the surface of the threat sphere if an acceleration equal to the surface gravitational acceleration of the Earth were constantly acting along the line joining the satellite and the threat. This acceleration was chosen on the grounds that it would always be greater than the actual net acceleration between the spacecraft. The relative state at the subsequent time was used to calculate the time of a further check in the same way. The process was repeated both forward and backward in time until the time from TCA was greater than 4000 seconds (about 67 minutes). No second close approach was ever found.

IV. Limitations and Numerical Problems

In this section the deficiencies of the algorithm and of its computer implementation are discussed. Certain limitations are described: the accuracy of the astrodynamic model and the handling of very eccentric orbits and very early maneuver times. Then some problems are described that were encountered concerning the choice of coordinate axes, numerical singularities, and exponent overflows during computing. The last subsection covers the most difficult problem, that of slow convergence.

Astrodynamic Model

Simple two-body orbital dynamics was used without including any perturbations or the surface of the Earth. This was done only for ease of computation; the algorithms do not assume any particular model. Since the orbital trajectories in an avoidance problem are usually less than a complete orbit, the difference between real motion and two-body motion should be negligible in most cases. Probably the model used would be practical for all satellites except those at very low altitude and those near or beyond the moon; however, this question was not investigated.

Extreme Orbits

Also for ease of computation, certain types of orbits

were excluded from consideration. The major restriction on the satellite orbit was that it not be hyperbolic: the procedure used to calculate $\underset{\sim}{\Phi}$ involved taking the square root of the semimajor axis. However, this is not essential to the method used, since $a^{1/2}$ can be eliminated from the derivation by replacing Eq (3.9) with

$$\dot{f} = \frac{\mu^{1/2}}{r_0 r} x(\gamma S - 1) \tag{4.1}$$

(1.202) and Eq (3.14) with

$$\mu^{1/2} t = x^3 S + \frac{\underline{r}_0 \cdot \underline{v}_0}{\mu^{1/2}} x^2 C + r_0 (1 - \gamma S) \tag{4.2}$$

(1.196) and using

$$a^{1/2} \sin(\gamma^{1/2}) = x(1 - \gamma S) \tag{4.3}$$

The algorithms were considered to have diverged when a trial trajectory was hyperbolic, so hyperbolic evasive trajectories could not have been found even if they were optimal. However, since two elliptical trajectories were always found even when the evasive maneuvers were large, it does not seem likely that any optimal hyperbolic trajectories existed in the problems run. The interceptor was allowed to be in a hyperbolic orbit; the only restriction was that its velocity be less than 200 kilometers per second.

Very Early Maneuvers and Multiple Revolutions

Because the orbit prediction algorithm as coded did not do well over long time spans, an upper limit of 86,160 seconds (about one sidereal day) was imposed on the time between maneuver and interception. This is probably much longer than the interval that would occur in any real situation. When the interval was smaller than this but still several times the orbital period of the attacker, another mathematical problem caused convergence to become erratic. Sometimes the optimization algorithm would produce a δt value comparable to the attacker's period. Then the program might iterate randomly, moving the evasive trajectory to various places around the attacker's orbit without getting back to the vicinity of the interception. It might also converge to an optimal closest approach on a revolution different from that of the attack. This could be easily recognized by the large difference between TCA and input intercept time. In any case, these problems were not considered to be of practical importance because an evasive maneuver probably would not be performed when the attacker was still several revolutions away.

Choice of Coordinate Axes

The program uses geocentric inertial cartesian coordinates for input, processing, and output. It was observed during program verification that when all input vectors were in the x-y plane, many elements of $\underline{\Psi}$ went to zero and

it became mathematically impossible for the algorithm to produce any $\delta\underset{\sim}{v}_o$ out of that plane. There was also a suspicion that numerical problems might arise when one or two coordinates of a vector got very close to zero. For these reasons, a subroutine was created to perform a coordinate transformation putting the intercept point in the middle of the first octant. The inverse transformation is done on the output, which is given in input coordinates.

Singularities and Overflows

If any of the 2 x 2 submatrices of the matrix $\underset{\sim}{E}$ (defined in Eq [2.33]) are singular, then certain intermediate results in the algorithms become undefined (i.e. Eqs [2.37] through [2.40] and [2.51] through [2.53]). No protection against this was put into the program and the problem never occurred; it would have caused the program to abort. On one occasion the denominator of Eq (2.60) became zero; the algorithm was modified to set $\delta\dot{x}$ equal to zero for any iteration on which this occurs. Another time the program aborted because of an exponent overflow while evaluating the numerator of the same equation, even though the value of $\delta\dot{x}$ was not unusually large or small. This problem was avoided by scaling down all the values used in the calculation. Program aborts besides these are probably possible, but none was encountered.

Speed of Convergence

It was found under most circumstances that all three algorithms converged quite quickly, usually in 5 to 15 iterations. The entire computer program would run from beginning to end, iterating to convergence from 9 initial guesses, in only a minute or so of wall clock time. However, three circumstances were found in which convergence became much slower. The first circumstance was the satellite at intercept time heading almost directly towards the Earth; the second was the satellite being in a very high circular orbit. The third was the interval between the maneuver and the intercept (which will be called the maneuver interval) being less than 10,000 seconds, or about 2 hours 47 minutes--this circumstance was of particular concern because it is short intervals that would probably be used in a real attempt at evasion. Fifty or more iterations were sometimes required in these cases, and it took the program tens of minutes to run. In extreme cases, the program limit of 100 iterations would be performed without convergence. Figure 4.1 shows how the number of iterations increased as maneuver interval went down. It is not understood why these circumstances should cause slow convergence.

In examining the behavior of the third algorithm (tangent trajectory, varying time) with a short maneuver interval, it was found that the ρ and ξ functions (representing the distance and tangency constraints) and the time of flight

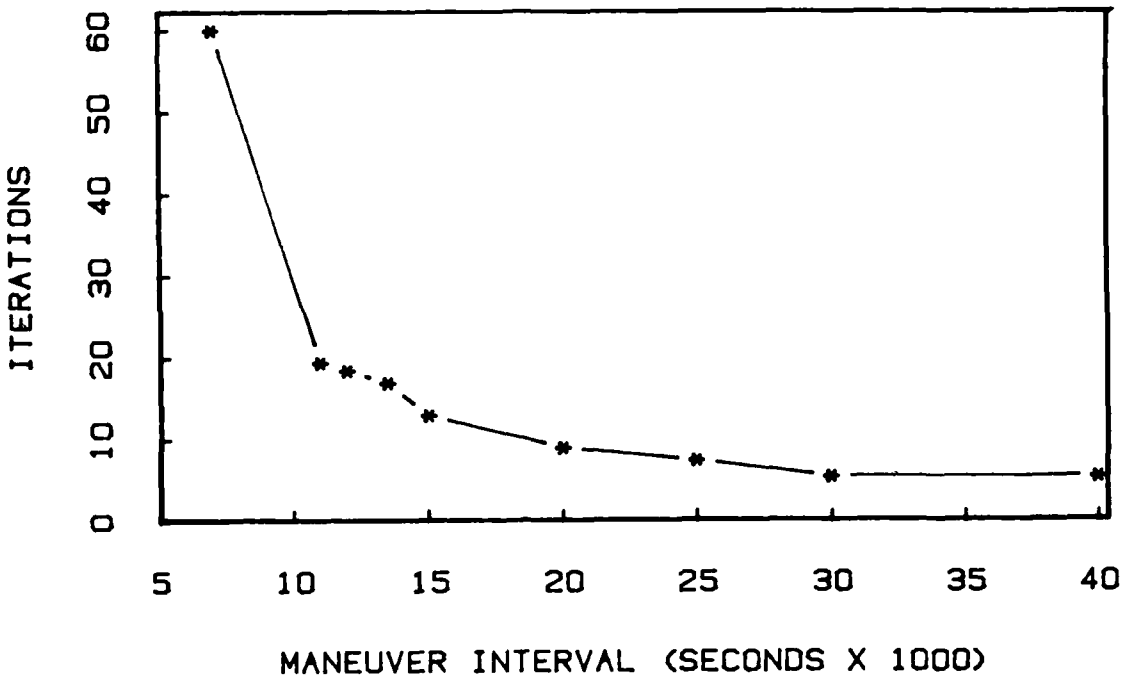

Figure 4.1. Iterations vs. Maneuver Interval

variable δt were brought within their convergence limits fairly quickly, usually within 10 iterations. The components of $\delta \underset{\sim}{v}_0$, on the other hand, converged much more slowly, and all at the same rate. The correction for each component was smaller at every iteration, but only by 10% to 40%, and it was always of the same sign. Furthermore, the trajectory end positions occupied successive points for approximately 5 degrees around a great circle of the threat sphere normal to the relative velocity vector. The situation is illustrated in Figure 5.2, in which trajectory AB represents the best path after the tenth iteration; it is tangent at B and has there the relative velocity vector $\underset{\sim}{v}_{10}$. Thirty iterations later, the tangency point is C and

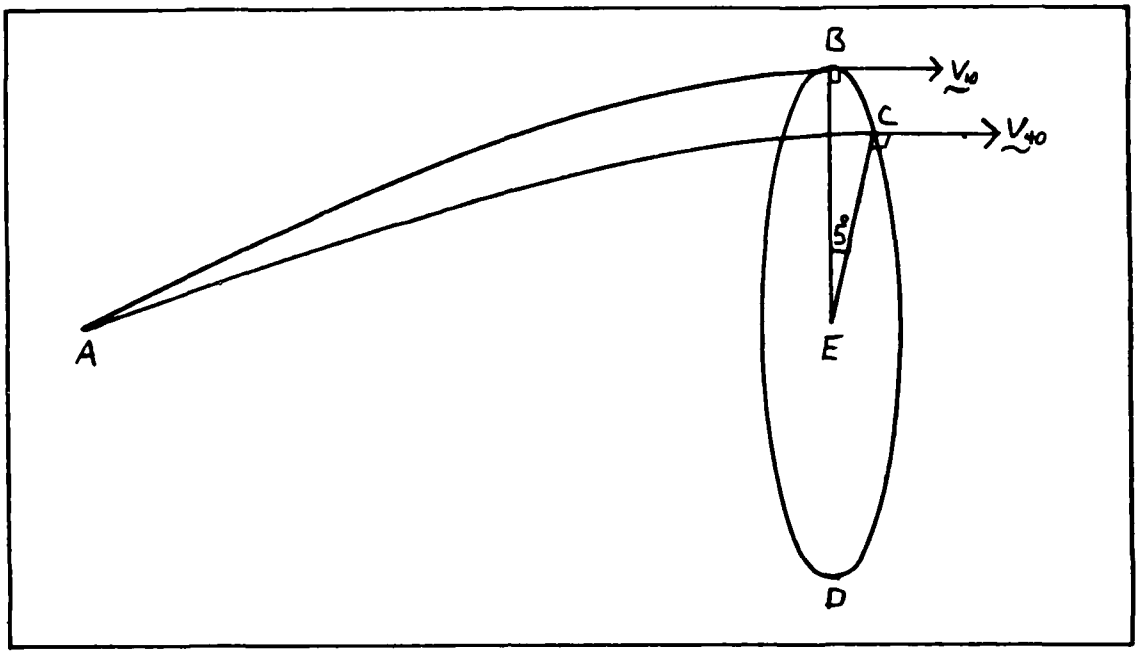

Figure 4.2. Locus of Trajectory End Points

the relative velocity vector is $\underset{\sim}{V}_{40}$. All the tangency points in between have been on arc BC of circle BCD, which is a great circle of the threat sphere centered at E. The conclusion of this was that although the algorithm works well in finding the great circle on which the optimal point of tangency lies, it is inefficient in moving around the circle to that point.

An attempt was made to improve convergence by reducing the degrees of freedom of the problem. Once the great circle was located, a different algorithm was used that allowed only points on the circle to be selected. The algorithm was otherwise similar to the algorithms in Section II. When this algorithm converged, its answer was turned over to the original procedure for final optimization.

This scheme performed somewhat worse than the original algorithm by itself.

The next approach involved multiplying the $\delta\underset{\sim}{v}_0$ corrections by an arbitrary constant to speed convergence. This approach was more successful. The constant was accepted by the program as part of the input. If three iterations in a row produced less than a 50% reduction in the magnitude of $\delta\underset{\sim}{v}_0$, the corrections on the last iteration were multiplied by the constant. If convergence was still slow after five more iterations, the factor was applied again; this procedure gave better results than using the factor on every iteration. By trial and error a factor could be found for every situation than produced convergence in 15 to 20 iterations. When the maneuver interval was very short the best factor was in the hundreds; Figure 4.3 shows how the best convergence factor increased as maneuver interval decreased.

As mentioned in Section III, the slow convergence of the algorithm had an effect on the selection of convergence criteria. It was found that when convergence was slow, different initial guesses converged on answers that were different only in their least significant figure. The convergence criterion for $\delta\underset{\sim}{v}_0$ was made more stringent by a factor of 10, and the two answers merged into one. Some particularly slow problems still reported convergence on not quite identical answers, so for them the limit was reduced by another factor of 10. Even then, the smallest

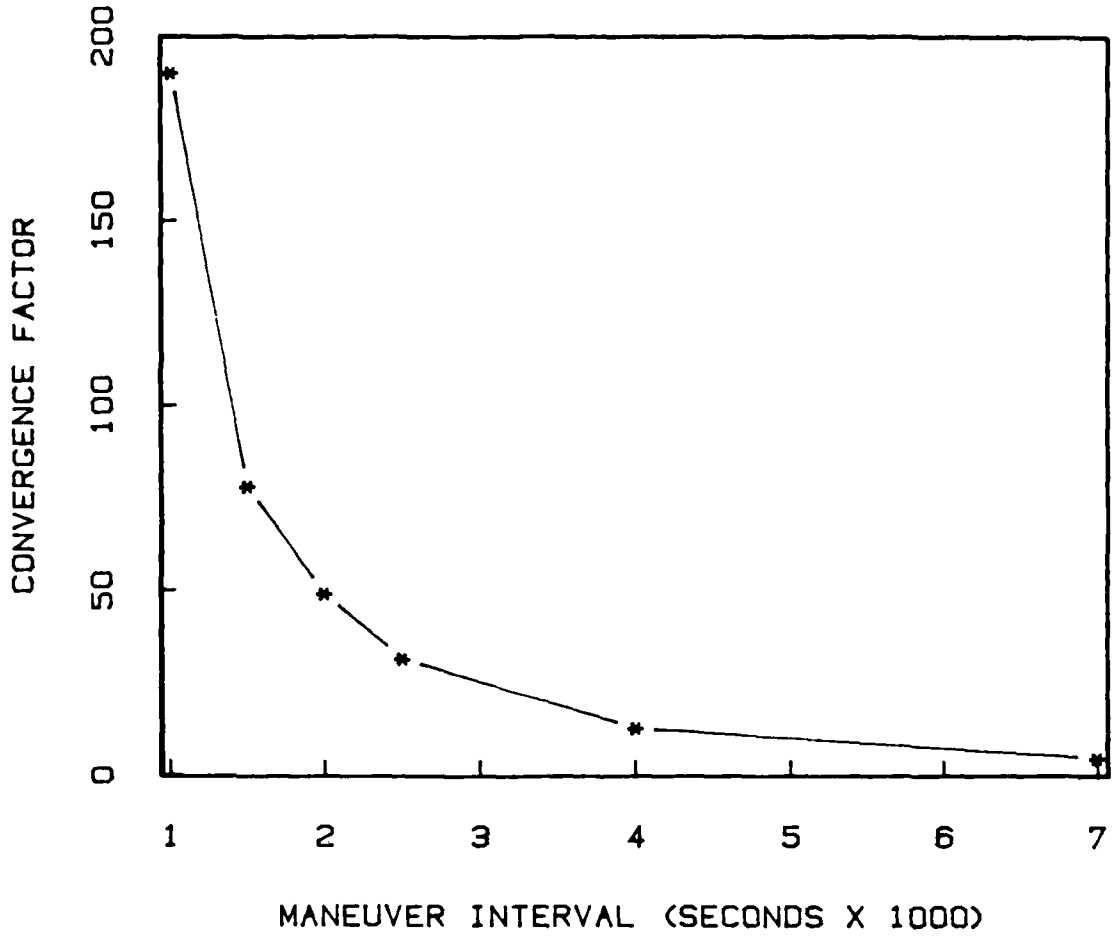

Figure 4.3. Factors Used for Short Maneuver Intervals

maneuver interval attempted (8 minutes 20 seconds) still resulted in multiple listings of the same essential answer.

V. Results

To add concreteness to what has been said about the program's input and output, this section begins with a description of the formats used. Then several evasion problems of special interest are examined. The first four feature maneuvers twelve hours before a geosynchronous interception; these cases are valuable both as examples and as aids in program validation. Maneuvers six hours before the intercept are then examined, followed by a maneuver to avoid a minimum energy interception. A problem taken from a realistic scenario is described in detail and then used as a standard of comparison. The section closes with an analysis of how maneuver size changed as each parameter of the standard interception was independently varied.

Sample Input and Output

Figure 5.1 shows the program's input in the format in which it lists it. First the satellite's state vector is given; the epoch time of the vector is in seconds from an arbitrary reference and can be any time within a day of the maneuver and the intercept. It was usually convenient to take the intercept time as the reference, as in the figure. The state vector of the threat follows; if the velocity is null the threat is treated as fixed. The next item is the threat sphere radius, followed by the intercept time in

```
EVASIVE MANEUVER PROGRAM


Satellite state vector at
t =       Ø.     seconds:       x                    y                    z

   Position (km):          42162.862               Ø.                   Ø.
   Velocity (km/sec):          Ø.                  3.Ø747107            Ø.

Threat state vector at
t =       Ø.     seconds:

   Position (km):          42162.862               Ø.                   Ø.
   Velocity (km/sec):          Ø.                  2.5ØØØØØØ            Ø.

Required keep-out distance:              5ØØ.ØØØ kilometers
Intercept expected at  t =                 Ø.    seconds
Maneuver at            t =           -43Ø8Ø.ØØØ seconds
Trace display code:                        Ø
Time variation allowed:                    t
Tangency constraint imposed:               t
Convergence factor:                        1.ØØØ
```

Figure 5.1. Sample Program Input

seconds from the reference. This time is the trajectory end time if time of flight is fixed and is used as an initial guess at time of closest approach if time of flight is free. The maneuver time is given next; this time is always fixed. The next input variable is an integer that governs the printing of intermediate results. The following two items are logical variables that control whether time of flight is fixed or allowed to vary and whether or not the evasion trajectory must be tangent to the threat sphere; together these variables govern which of the three algorithms is used. The final input item is the factor that will be used to increase every fifth iteration's corrections if convergence is slow.

Figure 5.2 shows how the program presents its output. For each of the locally optimal solutions, first the total magnitude of the required maneuver and the trajectory end time are given. This time will be in seconds from the same reference time that was used in the input. It will be the time of closest approach if time is allowed to vary and the same as the input intercept time otherwise. Following this, the cartesian components of the evasive maneuver are given. The last six lines contain three state vectors at trajectory end time, all in kilometers and kilometers per second. The first two are the inertial geocentric states of the satellite and of the threat; the third is the inertial state of the satellite relative to the threat. The globally optimal solution is selected manually by comparing

```
SOLUTION NUMBER  1

   Delta-V total magnitude:                  0.0405636 km/sec
   Trajectory End Time (TET):            -6897.284     seconds

                          x                    y                   z

   Delta-V (km/sec):       0.0320138          0.0249103          0.

   TET Position:       37297.50          -16320.64              -0.00
   TET Velocity:           1.2746725         2.8898677          -0.0000000
   TET Threat Pos:     36829.57          -16496.81               0.
   TET Threat Vel:         1.5458469         2.1696049          -0.0000000
   TET Sat Rel Pos:      467.93              176.17             -0.00
   TET Sat Rel Vel:       -0.2711744         0.7202628          -0.0000000


SOLUTION NUMBER  2

   Delta-V total magnitude:                  0.0071285 km/sec
   Trajectory End Time (TET):             1614.345     seconds

                          x                    y                   z

   Delta-V (km/sec):      -0.0009245         -0.0070683          0.0000000

   TET Position:       42366.15            3959.34               0.
   TET Velocity:          -0.2863693         3.0402290          0.0000000
   TET Threat Pos:     41870.68            4026.53               0.
   TET Threat Vel:        -0.3619846         2.4826348          0.
   TET Sat Rel Pos:      495.46             -67.19               0.
   TET Sat Rel Vel:        0.0756152         0.5575942          0.0000000
```

Figure 5.2. Sample Program Output

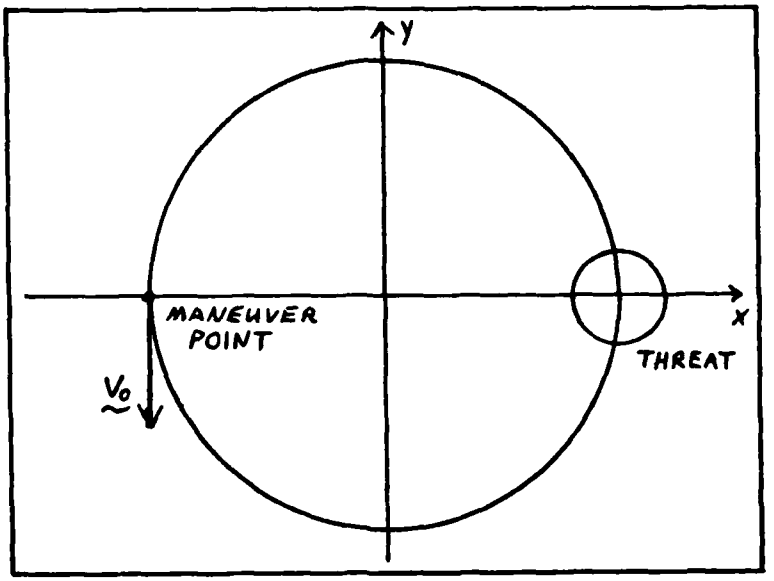

Figure 5.3. 12-hour Geosynchronous Maneuver

the sizes of the two maneuvers.

Maneuvers 12 Hours before a Geosynchronous Interception

An intercept situation with a fixed threat was run with each of the three algorithms, then the threat was given motion and a fourth run was made. The results illustrate how the required maneuver changes with the various constraints. They also validate the proper operation of the algorithms. The situation used is shown in Figure 5.3 and was that of the input in Figure 5.1: geosynchronous orbit in the x-y plane, 500-kilometer threat where the orbit crosses the x-axis, and maneuver performed half an orbit away. At maneuver time the satellite is on the negative x-axis and moving in the negative y direction; at the intercept it is on the positive x-axis and moving in

Table 5.1. No Tangency, Fixed Time, Fixed Threat

	Solution 1	Solution 2
Impulse Magnitude (m/sec)	3.343	3.351
x-component	1.149	-1.158
y-component	3.140	-3.145
Final Relative Position (km)		
x-component	-174.2	170.5
y-component	468.7	-470.0

the positive y direction.

No Tangency, Fixed Time, Fixed Threat. The first run looked for a trajectory ending anywhere on the surface of a fixed threat sphere at a fixed time. The two solutions are given in Table 5.1 (z-components were all zero and are omitted). Solution 1, which is slightly optimal, is mostly retrograde and results in a trajectory that flies through the threat sphere before the intercept time. Solution 2 is mostly prograde and flies through the threat sphere after the intercept time. Note that the two solutions use nearly opposite maneuvers and end at nearly opposite sides of the threat sphere.

Tangency, Fixed Time, Fixed Threat. The next run used the same input, except that one logical input was changed to impose the tangency constraint. The results are in Table 5.2. The tangency constraint is very expensive: the maneuvers required here are seven times larger than those of the previous case. The two solutions are still very similar in magnitude and nearly opposite in direction. The two tangency points are also still on nearly opposite sides

Table 5.2. Tangency, Fixed Time, Fixed Threat

	Solution 1	Solution 2
Impulse Magnitude (m/sec)	23.459	23.204
x-component	-21.587	21.367
y-component	9.184	-9.049
Final Relative Position (km)		
x-component	-500.0	500.0
y-component	-3.4	-3.6

Table 5.3. Tangency, Varying Time, Fixed Threat

	Solution 1	Solution 2
Impulse Magnitude (m/sec)	9.184	9.048
x-component	0.	0.
y-component	9.184	-9.048
Final Relative Position (km)		
x-component	-500.0	500.0
y-component	0.	0.
Time of Closest Approach	-382.6	383.7

of the threat sphere. They are almost on the x-axis, one being on the earthward side (inside) and one on the far side (outside). Solution 2, which passes on the far side, is optimal.

Tangency, Varying Time, Fixed Threat. The results of allowing time of flight to vary are shown in Table 5.3. It was expected that the extra degree of freedom in time would result in smaller maneuvers, and they were smaller by about 60%. It was also expected that the two optimal trajectories would be ellipses aligned along the x-axis. As shown in Figure 5.4, the maneuver point A would then be the apogee of the inner trajectory and the perigee of the outer trajectory. The tangency points would be at perigee B and at apogee C, respectively. As can be seen in the table,

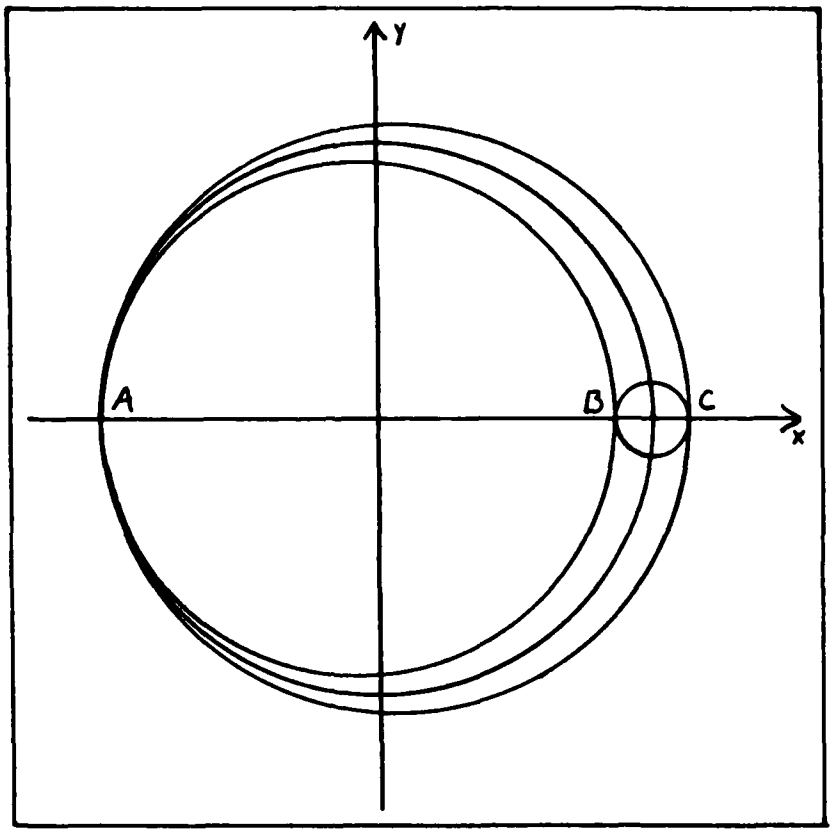

Figure 5.4. Tangent Ellipses with Varying Flight Times

this was the result. This case was important in validating the program, since the maneuver sizes could easily be checked manually. Note that here the maneuvers and the end positions have become exactly opposite. Solution 2 flies on the outside of the threat and is optimal; since the larger ellipse has the longer time of flight, the closest approach for this solution occurs after the nominal intercept time. (In all the runs that were made, it was usually found to be the case that one of the two solutions passed on the inside and the other on the outside of the threat,

Table 5.4. Tangency, Varying Time, Moving Threat

	Solution 1	Solution 2
Impulse Magnitude (m/sec)	40.564	7.128
x-component	32.014	-0.924
y-component	24.910	-7.068
Final Relative Position (km)		
x-component	467.9	495.5
y-component	176.2	-67.2
Time of Closest Approach	-6897.3	1614.3

and that the outside trajectory was optimal.)

Tangency, Varying Time, Moving Threat. In the last of this set of runs, the threat was put in a coplanar elliptical orbit and was at apogee at the expected intercept. This is the case shown in Figure 5.1 and Figure 5.2; the results are condensed in Table 5.4 for comparison. It was expected that the motion of the target would create opportunities for more optimal trajectories than were found with the fixed threat. Solution 1 turned out to be over four times worse, but Solution 2 showed an improvement. This was a case in which the two locally optimal solutions were quite different. Solution 1 has a large radial component and passes the threat almost two hours before the intercept time. Solution 2 is mostly prograde and results in a higher, slower orbit that passes the threat about 27 minutes after the latter's perigee. Note that the optimal maneuver here is only a little more than twice as large as the optimal maneuver in the first case, in which the threat and the time of flight were fixed but the tangency constraint was not imposed.

Table 5.5. 6 Hour Interval, Fixed Threat

	Solution 1	Solution 2
Impulse Magnitude (m/sec)	16.222	16.393
x-component	14.478	-14.693
y-component	-7.313	7.269
Final Relative Position (km)		
x-component	500.0	-500.0
y-component	-4.8	-4.7
Time of Closest Approach	110.2	-112.5

Maneuvers 6 Hours before a Geosynchronous Interception

A series of runs was made similar to those of the previous subsection but with the maneuver only a quarter of an orbit before the intercept. The last two of these were of some interest. The results of running the problem with the tangency constraint imposed and time allowed to vary but with the threat fixed are shown in Table 5.5, which should be compared with Table 5.3. The time until intercept has been halved and the maneuver size has increased by about 80%. The maneuver and the evasion ellipse are no longer aligned with the axes. A prograde maneuver of 18.18 meters per second would have created a perigee on the y-axis and been very nearly tangent to the threat sphere on the outside; the program found two better trajectories with rotated major axes.

The results with a moving threat are shown in Table 5.6. The threat here had the same orbit as that used for Table 5.4. Note that again the moving threat caused the two locally optimal solutions to move further apart and allowed a better globally optimal solution. The better

Table 5.6. 6 Hour Interval, Moving Threat

	Solution 1	Solution 2
Impulse Magnitude (m/sec)	15.415	17.383
x-component	13.326	-16.087
y-component	-7.749	6.585
Final Relative Position (km)		
x-component	497.7	-498.0
y-component	-48.3	-44.8
Time of Closest Approach	530.2	-641.6

solution is again the one that passes the threat after the original intercept time.

Minimum Energy Geosynchronous Interception

The requirements for avoiding a low-energy geosynchronous interception are also of interest. In this case the third algorithm (time free, trajectory tangent to sphere) was used. The situation was modeled by assuming that the threat was given a vertical velocity at the Earth's equator just great enough to carry it to geosynchronous altitude. The rotation of the Earth gives the attacker a transverse velocity of about 465 meters per second; this makes the attack trajectory an elongated ellipse. By equating angular momentum at the surface of the Earth and at apogee, one finds that apogee velocity is about 70.361 meters per second. Using a threat radius of 300 kilometers, a maneuver interval of 7000 seconds (1.94 hours), and the threat orbit described, the optimal avoidance maneuver is one of 39.6764 meters per second. The trajectory passes the threat on the outside about 5 seconds after the planned intercept. If

the maneuver interval is doubled to 14,000 seconds (3.89 hours), the required maneuver is less than half as big, being only 17.0532 meters per second. However, 14,000 seconds is almost half the attacker's orbital period, so the shorter interval probably allows a more realistic period for detection and tracking of the attack.

A Standard Interception

It was the writer's plan to include in the research a comprehensive survey of the effects of all applicable variables on maneuver size. Such a survey would be of practical interest, and it would also demonstrate that the program worked under a wide variety of conditions. The survey was to be accomplished by taking a case from a plausible scenario and varying each parameter independently. The following describes how the standard interception was chosen.

A satellite in a circular geosynchronous equatorial orbit was chosen as the target of the attack. This description fits a large number of military satellites. It also has the virtue of simplicity. An attack by direct ascent from the surface of the Earth was chosen as a likely near-term threat. The attacker might be expected to minimize the energy of his trajectory in order to maximize his payload, so the threat was given an orbit with apogee at the intercept point. However, the attacker would probably not be free to choose the position of his launch site, so

Table 5.7. Summary of Geosynchronous Orbit Cases

	Maneuver Interval (hrs)	Tangency	Varying Time	Threat Radius (km)	Threat Motion	Minimum Impulse (m/sec)
1.	12	No	No	500	Fixed	3.343
2.	12	Yes	No	500	Fixed	23.204
3.	12	Yes	Yes	500	Fixed	9.048
4.	12	Yes	Yes	500	Coplanar	7.128
5.	6	Yes	Yes	500	Fixed	16.222
6.	6	Yes	Yes	500	Coplanar	15.415
7.	1.94	Yes	Yes	300	Coplanar	39.676
8.	3.89	Yes	Yes	300	Coplanar	17.053
9.	1.94	Yes	Yes	300	Inclined	39.648

the coplanar minimum energy interception described above was not suitable. A launch site in the middle northern latitudes would be plausible, so an orbital inclination of 45 degrees was chosen. An apogee velocity of one kilometer per second was selected as a round number that left perigee within the Earth. The threat radius was fixed at 300 kilometers. To find a reasonable maneuver interval, the threat orbit period of 9.2 hours was considered. Allowance was made for the fact that the attacker would start at a point past perigee and would have to be detected and tracked, and an interval of about 2 hours (7000 seconds) was used. Finally, the third algorithm (time free, trajectory tangent to sphere) was chosen as the most likely to meet real mission requirements.

The minimum impulse for the standard interception is compared in Table 5.7 to all the cases discussed so far. The first through fourth lines describe the cases in which the maneuver was made halfway around the orbit; the fifth

and sixth give the results when the maneuver was made a quarter of the way around. Lines seven and eight represent avoidance of the minimum energy attack. The last line in the table gives the result of the standard interception, which was 39.6480 meters per second. This value was used as a basis of comparison as each variable in the interception was changed.

Variations on the Standard

Eleven parameters were varied in the standard interception:

1. Radius of the threat sphere
2. Maneuver interval
3. Attacker speed
4. Attacker orbital inclination
5. Attacker flight path angle
6. Satellite speed
7. Satellite flight path angle
8. Satellite orbital altitude
9. Intercept radial miss distance
10. Intercept in-track miss distance
11. Intercept cross-track miss distance

Each of these was varied over as wide a range as practical, while the other parameters were held as constant as possible. Maneuver size was plotted as a function of each of them. The plots are shown in Figures 5.5 through 5.16; the exact values are tabulated in the Appendix. The graphs are

not all on the same scale because a scale large enough to show the big variations would have made the small ones undetectable: some of the parameters affected maneuver size very strongly and others hardly at all. The following paragraphs describe how each plot was made and remark on some of their interesting features.

Radius of the Threat Sphere. Required miss distance was varied from 50 to 1000 kilometers. Figure 5.5 shows the plot. The variation was very strong and remarkably linear.

Maneuver Interval. The second parameter varied was the time between the maneuver and the interception. This was varied from 500 seconds (8 minutes 20 seconds) to 80,000 seconds (22 hours 13 minutes 20 seconds). The results up to 10,000 seconds are shown in Figure 5.6 and the remainder in Figure 5.7. Note that the two graphs have very similar exponential-type shapes even though very different vertical and horizontal scales are used. As expected, maneuver size decreased as the interval increased and was very large at short times. It was also at these short times that the program had the greatest difficulty converging. There was a small increase in required impulse for the longest maneuver interval, which was nearly as long as the orbital period of the satellite.

Attacker Speed. The magnitude of the attacker's velocity at intercept time was varied without changing the other components of its state vector. As the speed went

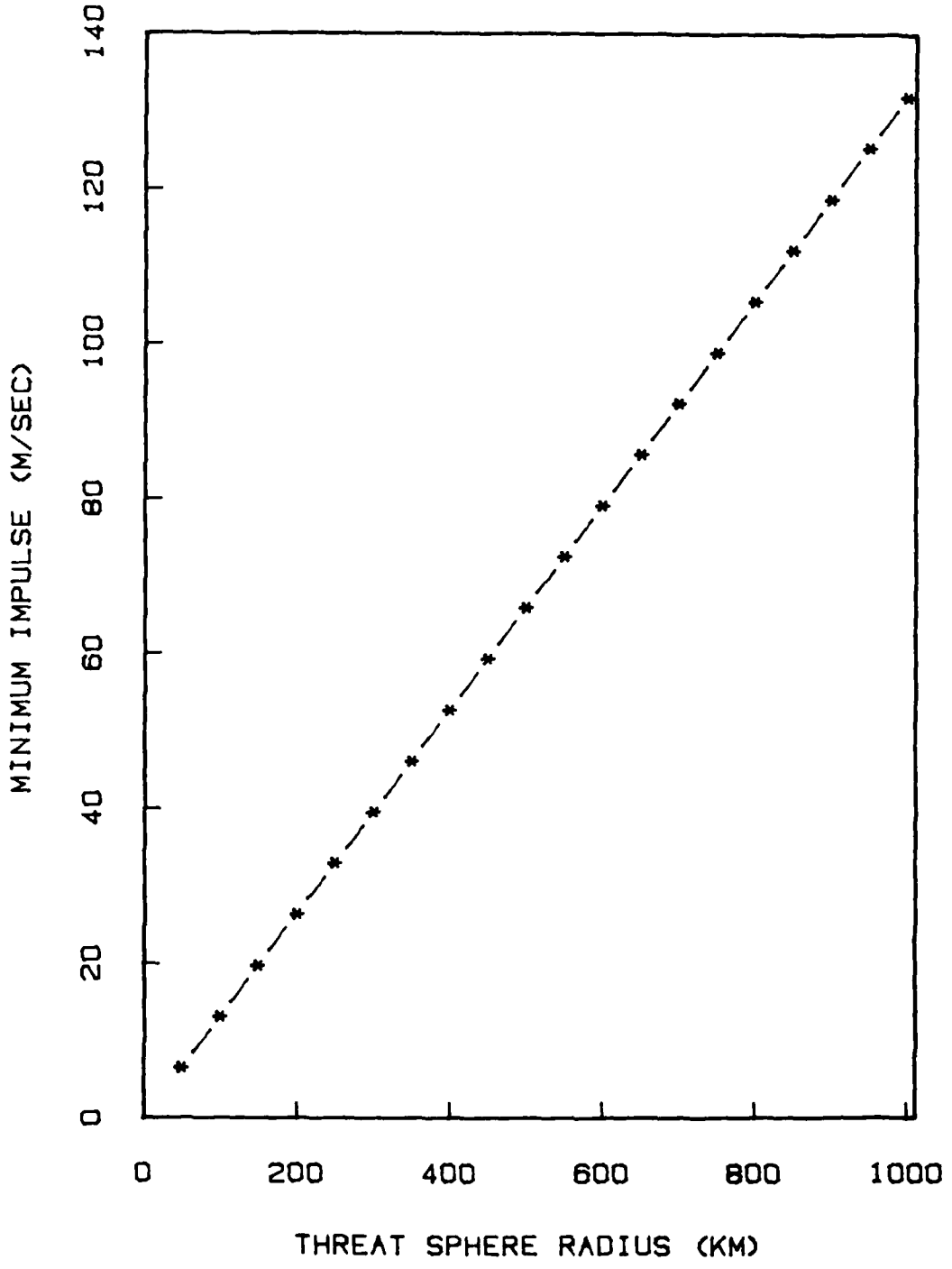

Figure 5.5. Impulse vs. Threat Sphere Radius

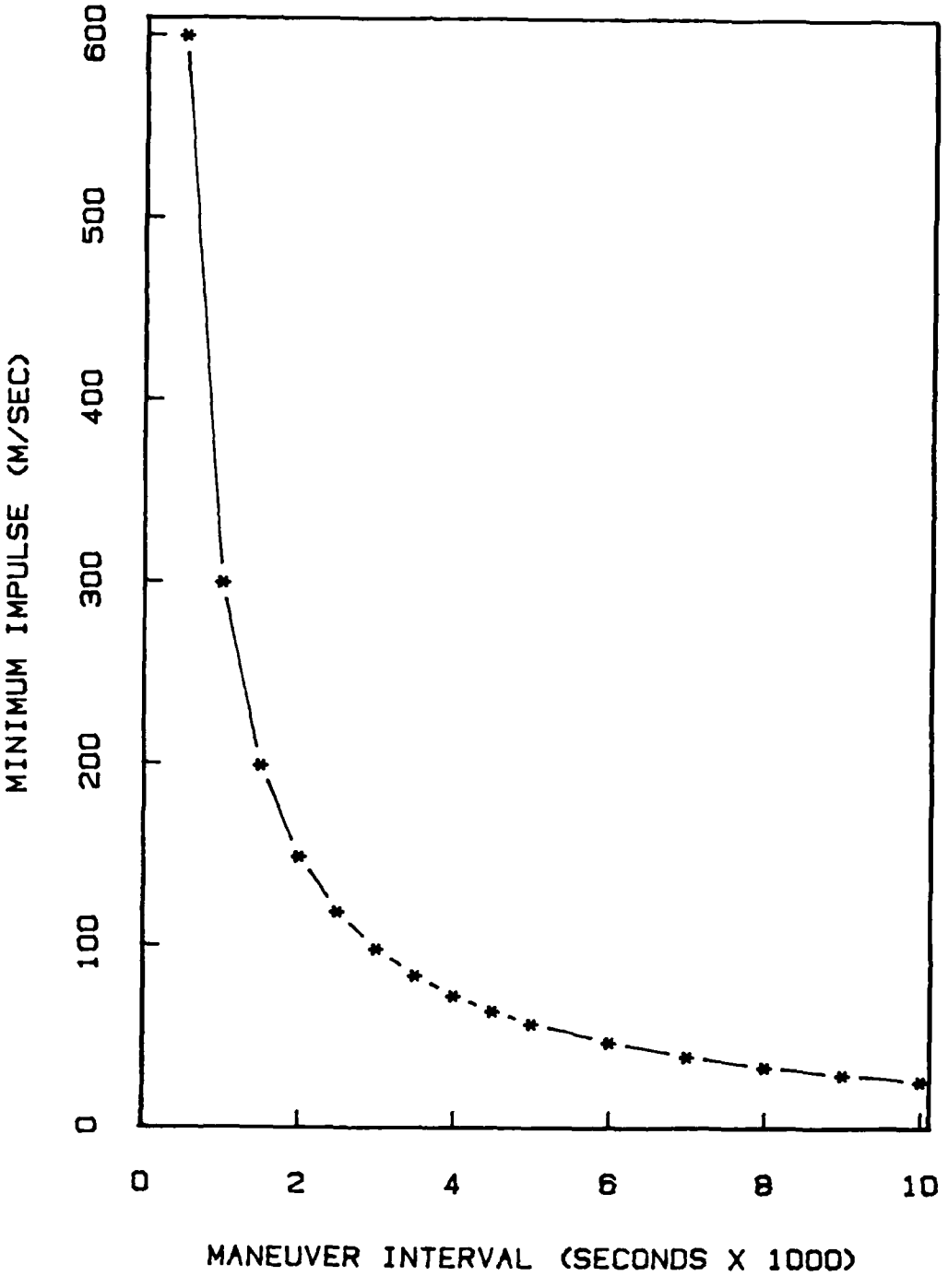

Figure 5.6. Impulse vs. Short Maneuver Intervals

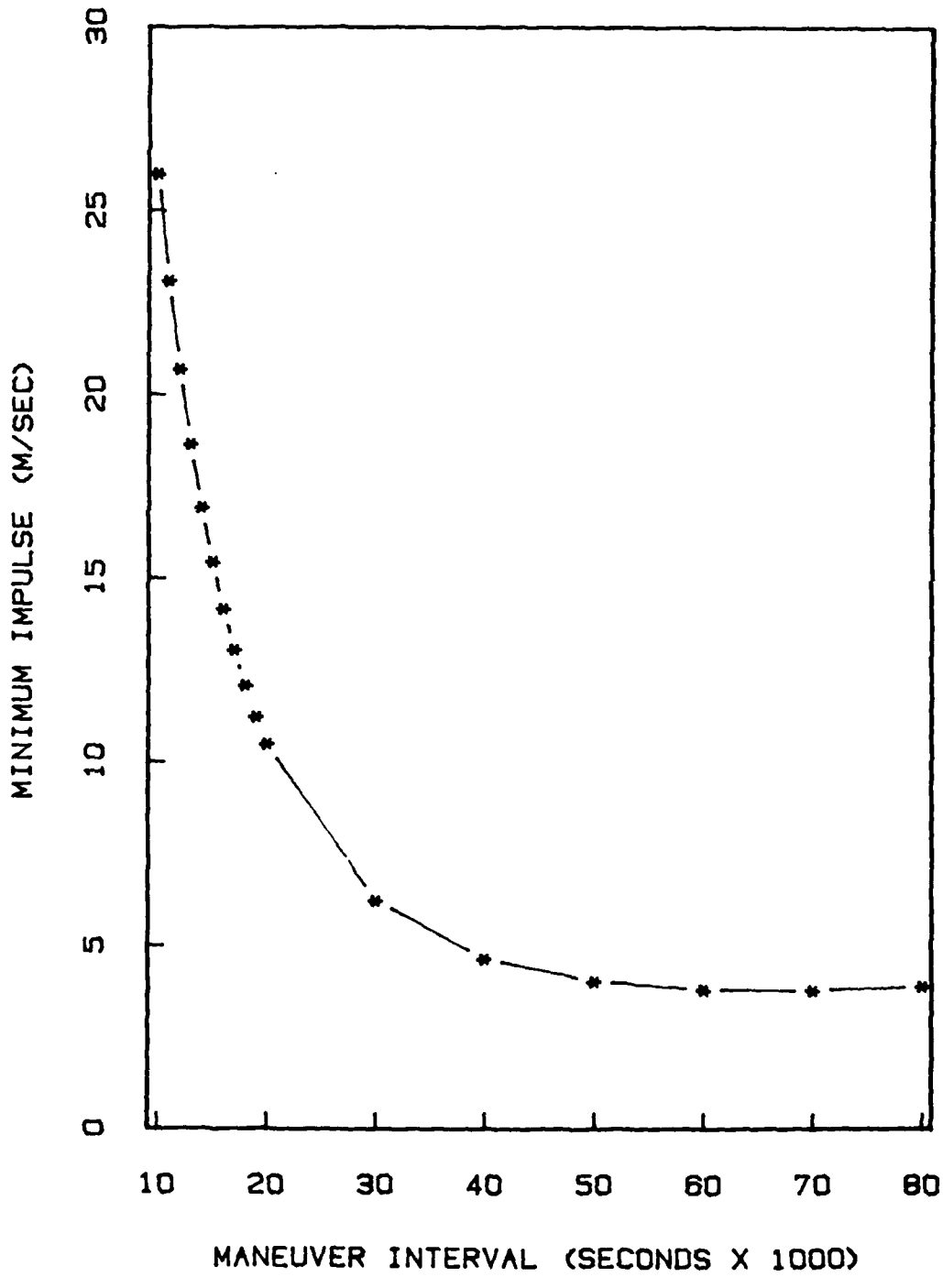

Figure 5.7. Impulse vs. Long Maneuver Intervals

from 0.25 to 5.00 kilometers per second, the intercept point went from being the apogee of a very elongated ellipse to the perigee of a very large ellipse and finally became the perigee of an hyperbola. The results are shown in Figure 5.8. It is interesting that maneuver size decreases smoothly as attack speed increases: a slower attacker is harder to avoid. Here again the last point reverses the trend of the rest of the graph. However, the total variation in this graph is very small, less than one percent. The encounter geometry is such that the satellite passes on outside of the threat up through the intercept at 3 kilometers per second; after that it passes on the Earth side.

Attacker Orbital Inclination. The azimuth of the attack had a very small effect on impulse size, with less than 4 centimeters per second separating the extremes. The results are in Figure 5.9. The evasive maneuver was greatest with an orbital inclination of 180 degrees, in which the threat was coming head-on in a retrograde orbit.

Attacker Flight Path Angle. A spacecraft's flight path angle is the angle of its velocity vector above the local horizon. In the standard interception both vehicles have a zero angle. Without changing its magnitude, the threat velocity vector was moved around in a circle covering all possible flight path angles; the corresponding graph is in Figure 5.10. The total variation here is somewhat greater than in the previous two graphs, being

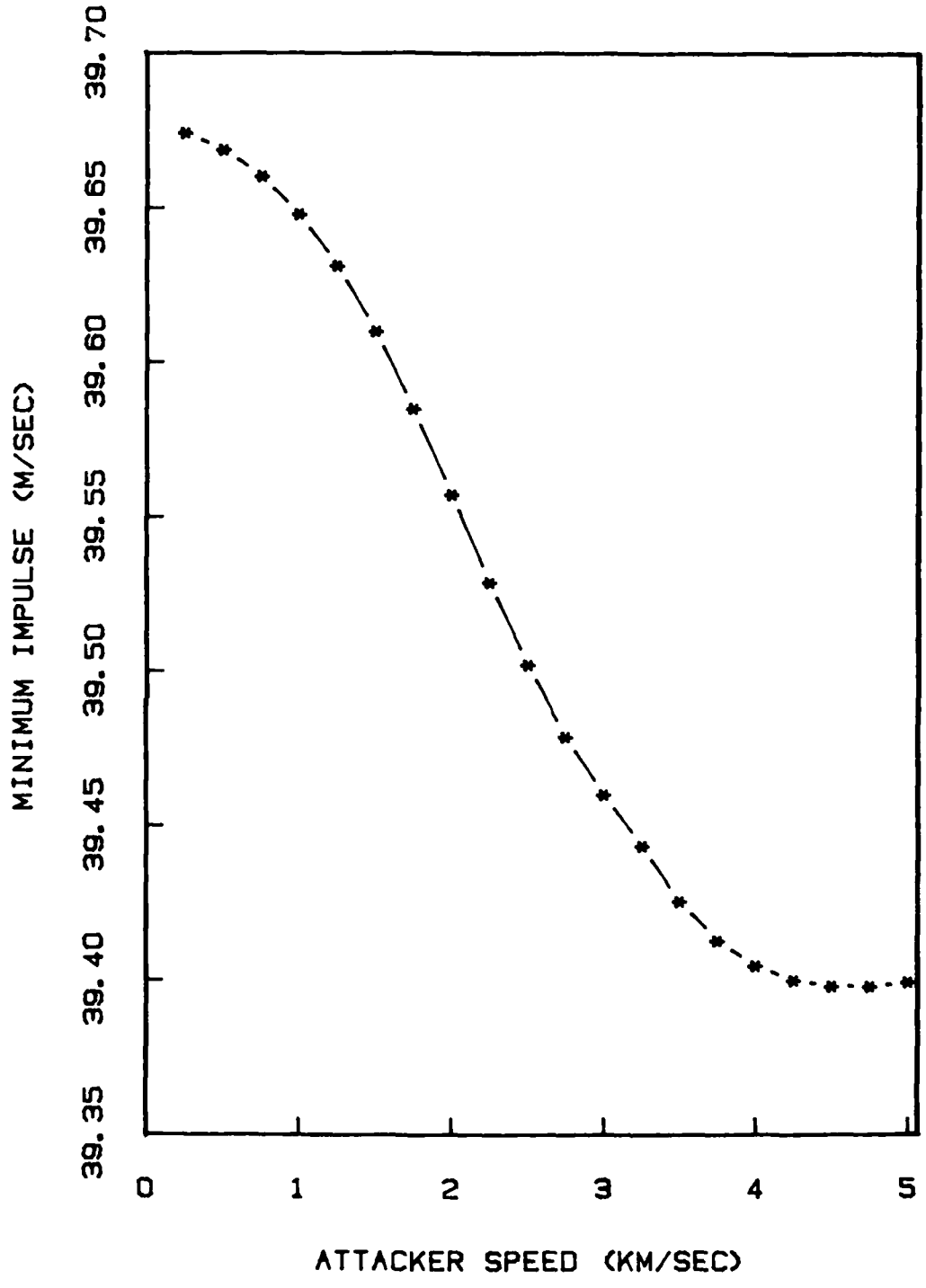

Figure 5.8. Impulse vs. Attacker Speed

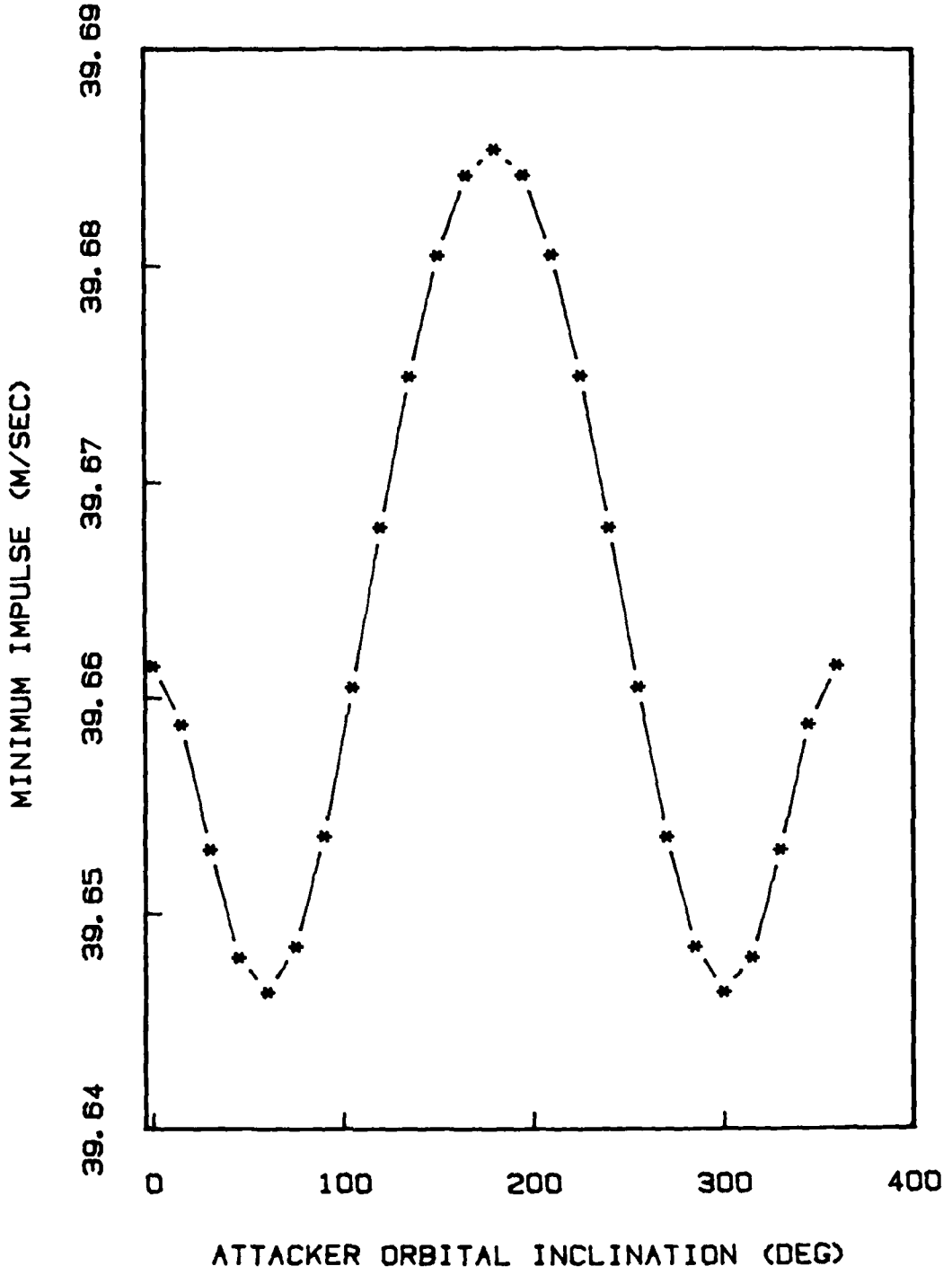

Figure 5.9. Impulse vs. Attacker Orbital Inclination

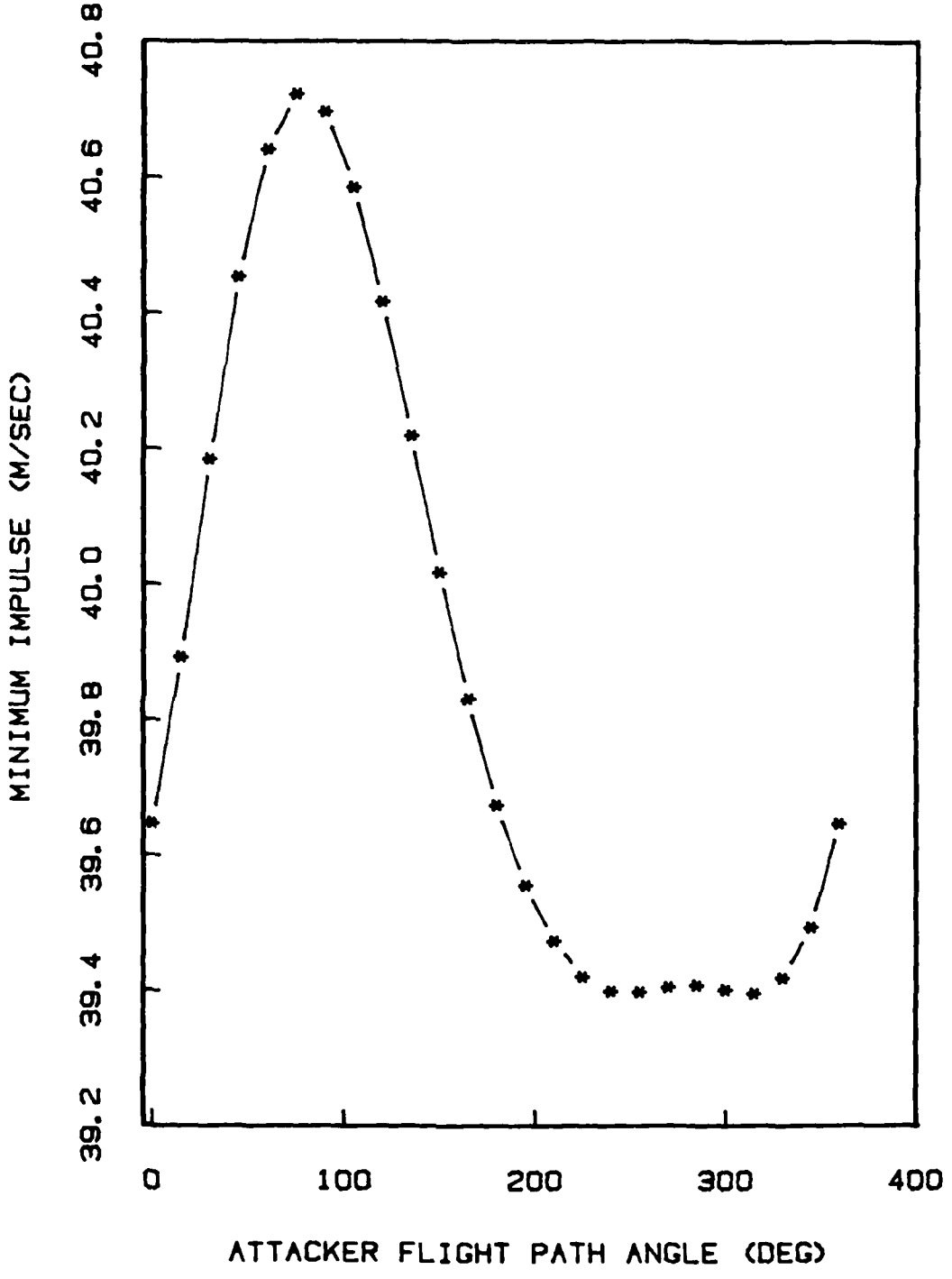

Figure 5.10. Impulse vs. Attacker Flight Path Angle

about 3.4%. There is a pronounced maximum where the attacker is coming almost directly up and a broad minimum where he is coming straight down. The minimum occurs because a small prograde maneuver makes the satellite arrive later and higher at the intercept point, exactly right for avoiding a falling threat. The same maneuver will meet a rising threat.

Satellite Speed. The magnitude of the satellite's velocity at intercept time was varied from 1.6 to 4.2 kilometers per second. The resulting orbits ranged from an eccentric ellipse with perigee very close to the atmosphere to something close to a parabola. Looking at Figure 5.11, one can see that the variation was nearly linear, although it was over a fairly small range (2.6%).

Satellite Flight Path Angle. In the standard interception the satellite was in a circular orbit with a flight path angle of zero. Keeping speed and orbital plane unchanged, this angle was changed through 360 degrees, so that the intercept point became a point first on the ascending part and then on the descending part of ellipses of varing eccentricity (including rectilinear trajectories), all ellipses having the same energy. Figure 5.12 shows that the variation was irregular in shape and over 30% in magnitude. There is a very strong peak when the satellite is going straight up (flight path angle of 90 degrees) followed by a steep drop to a minimum near 120 degrees. A second maximum that is broader and lower corresponds to the

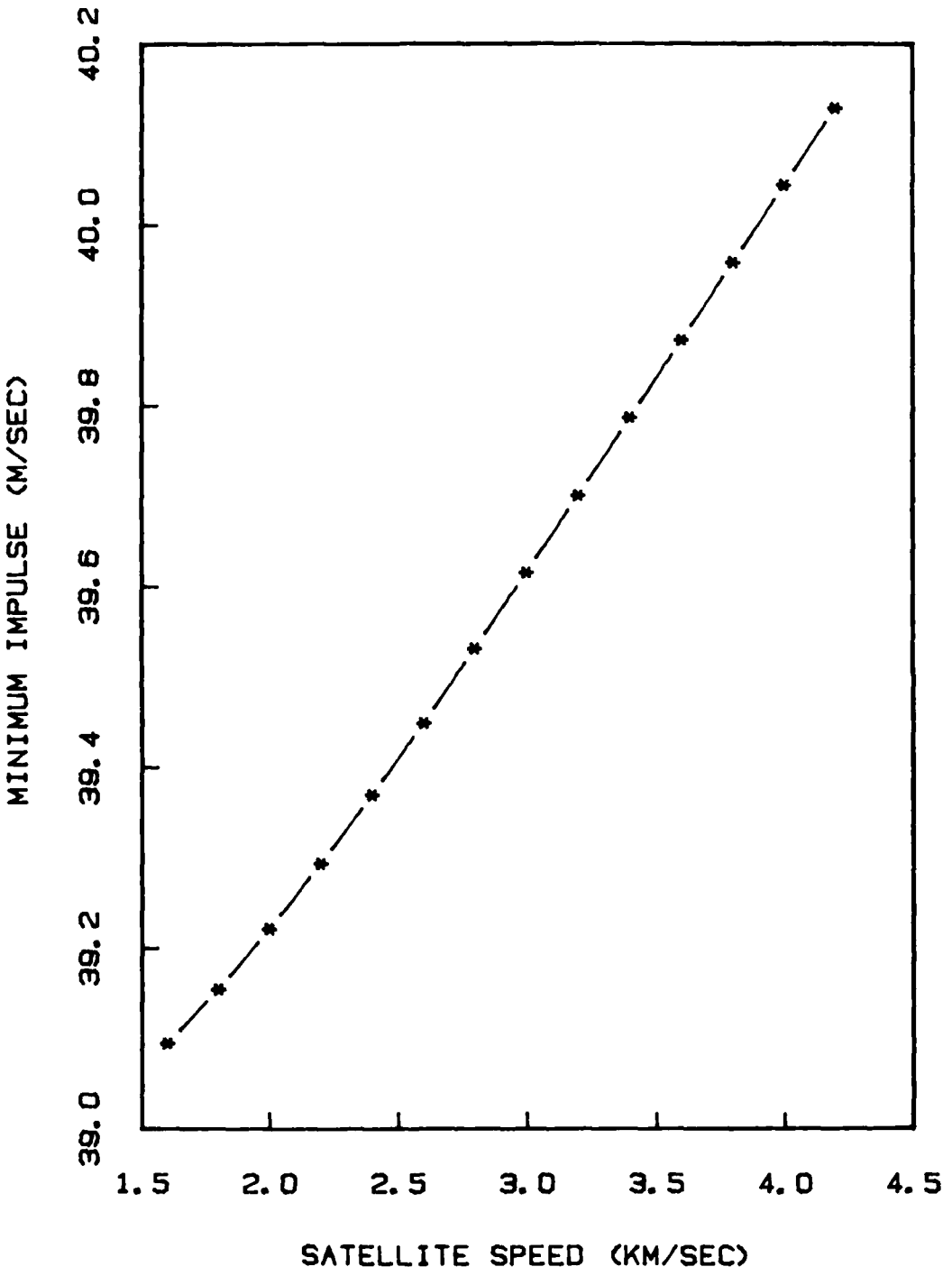

Figure 5.11. Impulse vs. Satellite Speed

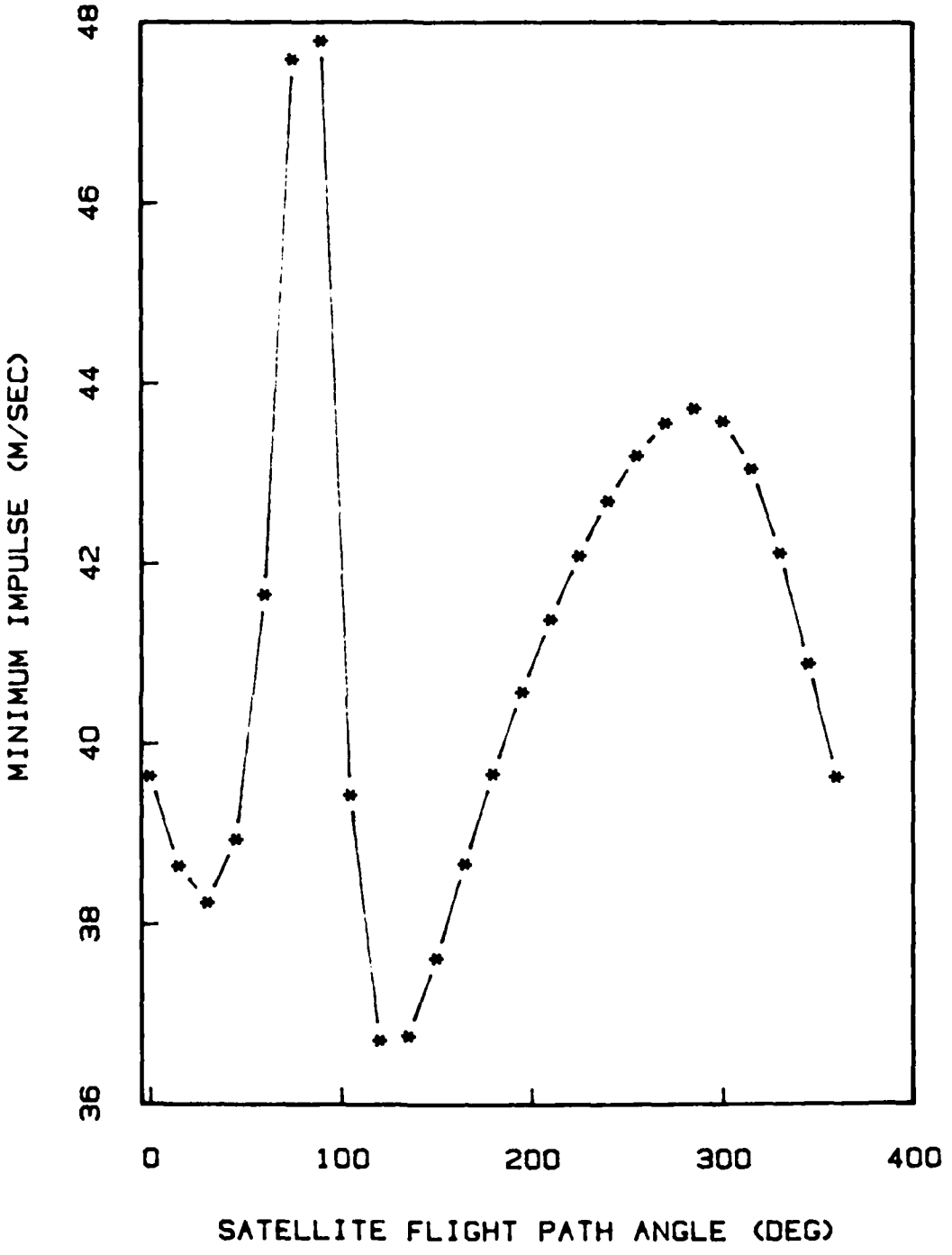

Figure 5.12. Impulse vs. Satellite Flight Path Angle

satellite falling nearly directly towards the Earth. This second peak was an area where convergence of the program became slow and convergence factors in the tens had to be used.

Satellite Orbital Altitude. The radius of the satellite's orbit was varied from 12,000 to 80,000 kilometers. Its orbital velocity was changed to keep the orbit circular. The attacker's velocity vector was not changed, so its orbit shape changed from case to case. The results are in Figure 5.13. With the exception of the first point, the trend is an ever-slower increase in maneuver size as altitude increases; the total variation here is over 54%.

Intercept Radial Miss Distance. All of the problems described so far have started with an interception that is a direct hit. The next set of runs to be considered varied the radial position of the threat at intercept time from 250 kilometers on the earthward side of the satellite to 250 kilometers on the far side. Figure 5.14 shows that maneuver size went down linearly as miss distance increased, and that misses on the inside and on the outside produced the same effect.

Intercept In-track Miss Distance. The position of the threat at intercept time was varied 250 kilometers in either direction along the satellite's flight path. The results are plotted in Figure 5.15. The plot does not go to zero when the miss distance approaches the keep-out range (300 kilometers) because both the satellite and the at-

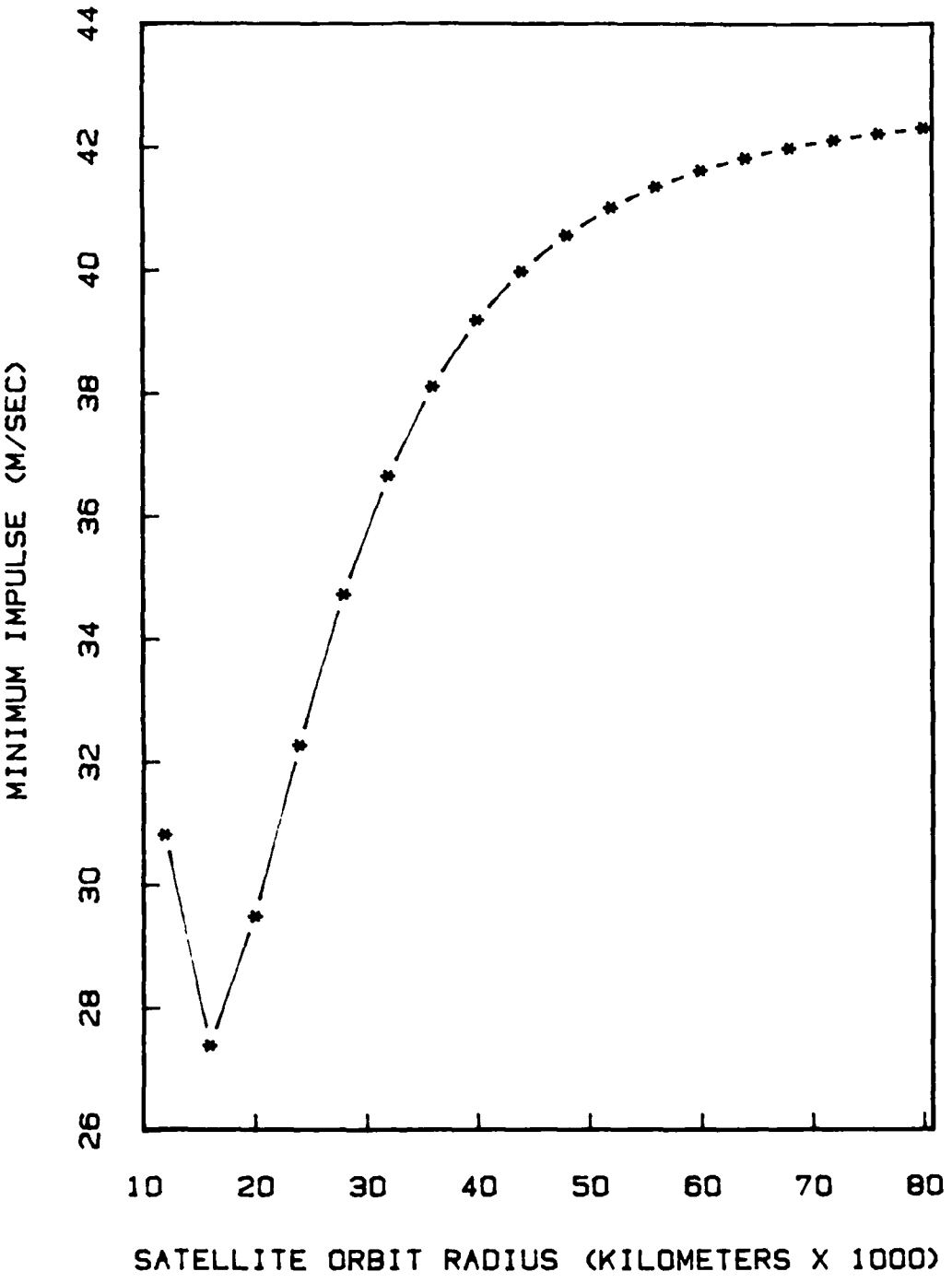

Figure 5.13. Impulse vs. Satellite Orbital Altitude

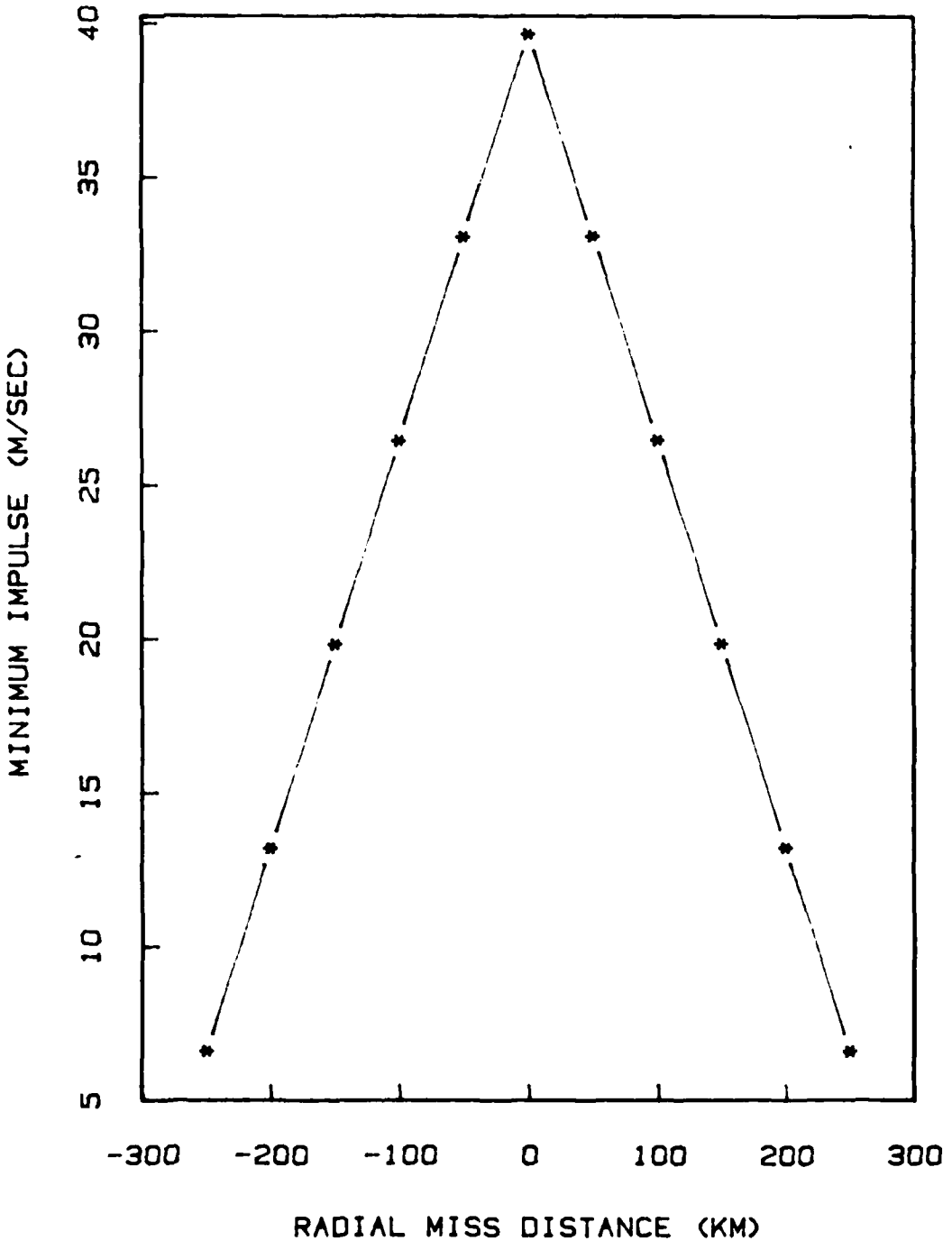

Figure 5.14. Impulse vs. Radial Miss Distance

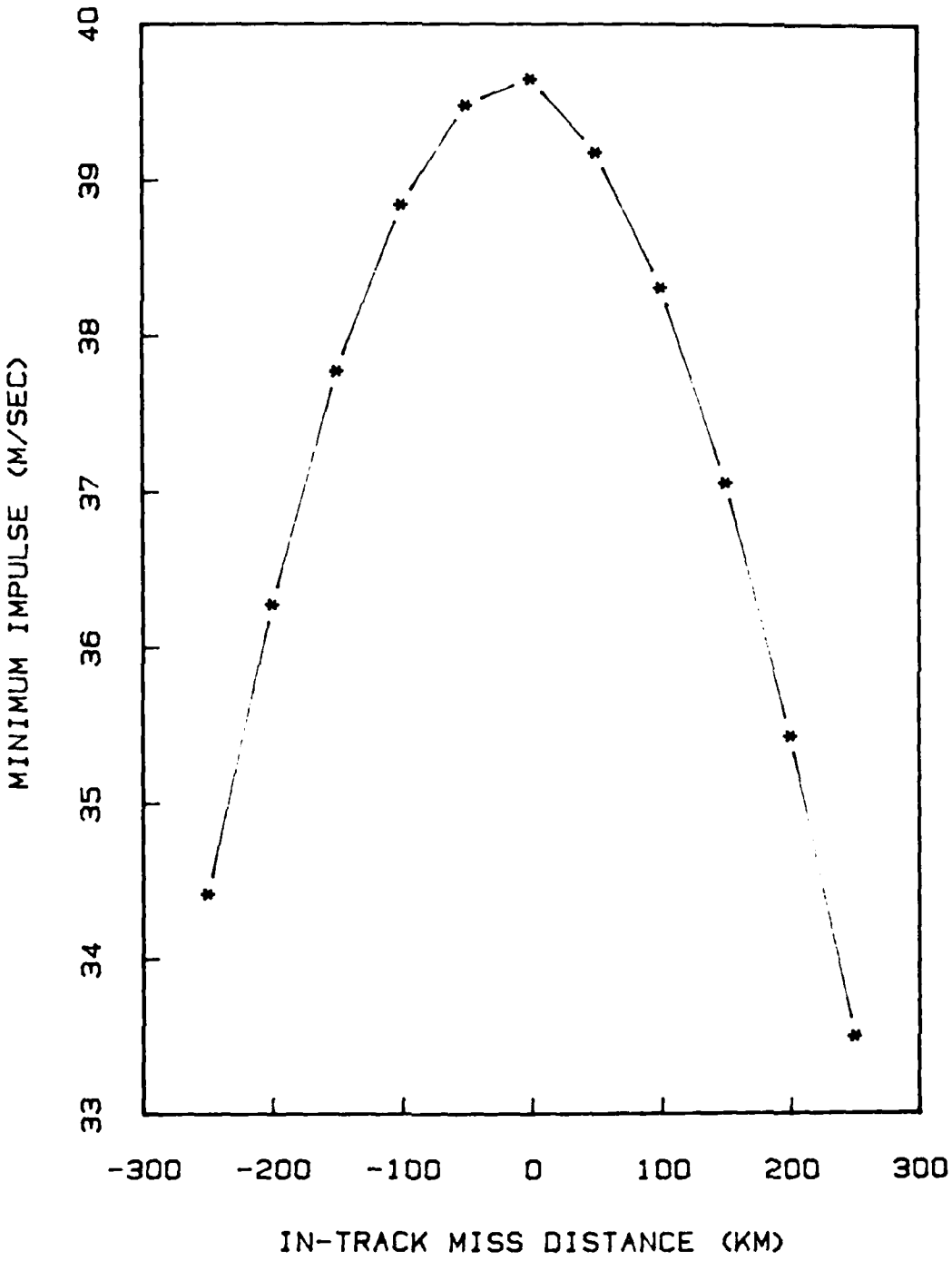

Figure 5.15. Impulse vs. In-track Miss Distance

tacker have large components of velocity in the in-track direction. Even if at the stated intercept time the satellite is near the surface of the threat sphere, the relative in-track motion of the spacecraft puts the satellite deep inside the sphere either before or afterwards. This means that the intercept time given in the problem statement is not the time of closest approach. If the in-track miss distance were made still larger, the maneuver would certainly go to zero.

Intercept Cross-track Miss Distance. The interceptor has a cross-track velocity component but the satellite does not. In the graph of variations along this axis (Figure 5.16), the peak is rounded because when the miss distance is small, the cross-track velocity of the attacker still causes a close approach before or after the intercept time. When the cross-track miss is over 100 kilometers, the high in-track speed of the satellite leaves the attacker behind before the latter's cross-track velocity can bring it near. As the miss distance increases beyond 100 kilometers, the required evasive maneuver drops linearly towards zero.

Summary. Table 5.8 summarizes the effects of all the parameters on maneuver size. The lowest and highest impulses are given for each variation, and the difference between them is expressed as a percentage of the lowest. The last column describes the general trend of each variation in one or two words.

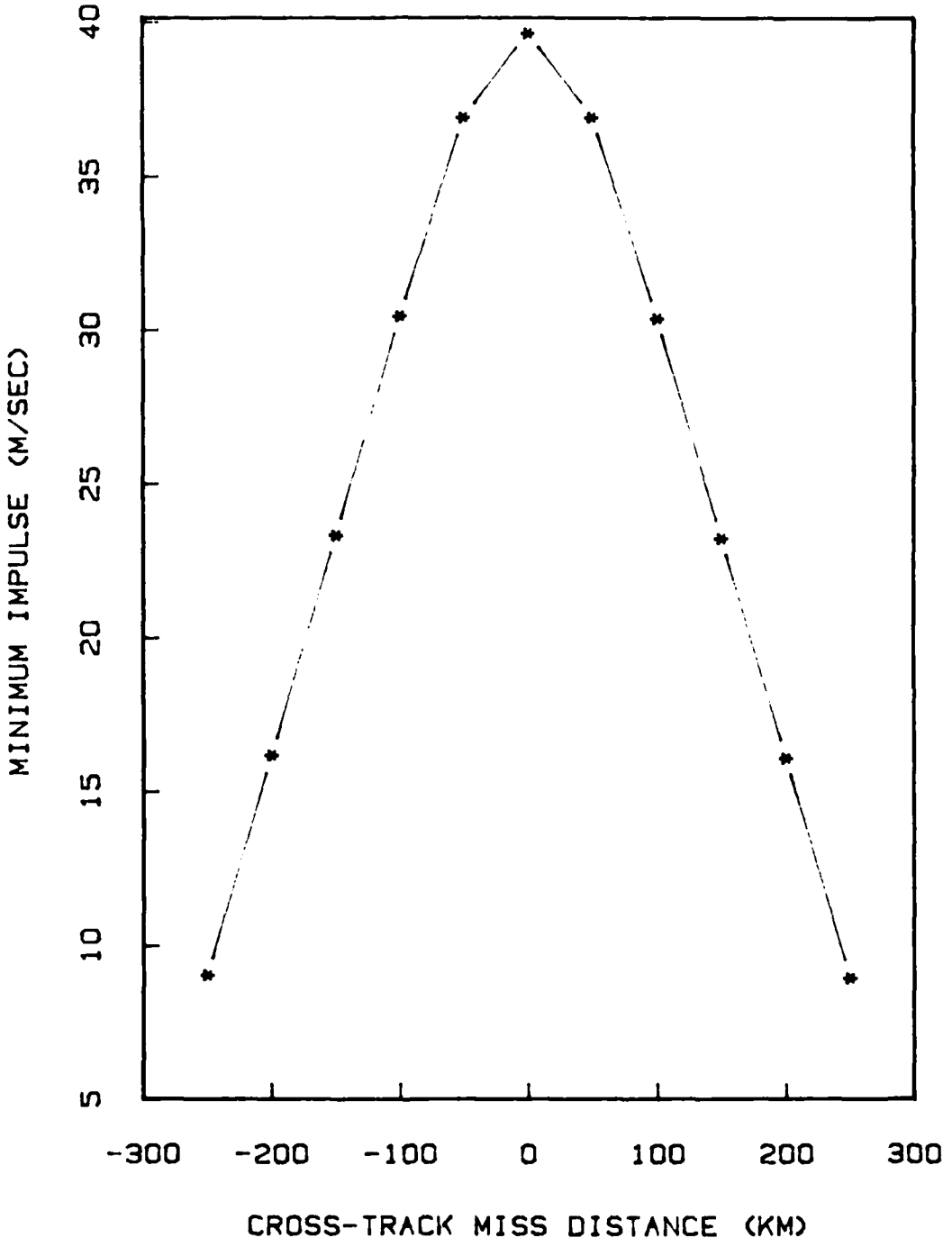

Figure 5.16. Impulse vs. Cross-Track Miss Distance

TABLE 5.8

Summary of Variations on the Standard Interception

Parameter Varied	Low Impulse	High Impulse	% Diff	General Shape of Curve
Sphere radius	6.612	132.010	1897%	Linear
Maneuver interval	3.932	599.756	15153%	Exponential
Attacker speed	39.398	39.674	0.70%	Cosine (half)
Attacker inclination	39.646	39.685	0.10%	Negative sinusoid
Attacker flight path angle	39.398	40.723	3.36%	Irregular sinusoid
Satellite speed	39.095	40.130	2.65%	Linear
Sat. flight path angle	36.709	47.801	30%	Irregular
Orbital altitude	27.397	42.323	54%	Logarithmic
Radial miss distance	6.615	39.648	499%	Lambda
In-track miss distance	33.503	39.648	18%	Rounded lambda
Cross-track miss distance	8.981	39.648	341%	Rounded lambda

VI. Conclusions

The goal of the research was to create and validate an algorithm that could calculate optimal impulsive orbital evasive maneuvers. This was accomplished. The algorithm is imperfect in that in some important situations a convergence factor must be found by trial and error. However, after a few trials the optimal solution could always be found. The thesis concludes with a review of the results of varying the standard interception, some remarks on the tactics of orbital evasion, and suggestions for further research.

Factors that Affect Maneuver Size

In the many variations that were made on the standard interception, some parameters had unexpectedly strong effects and others unexpectedly weak. It was not surprising that the lethal radius of the threat and the time of the maneuver had the strongest influence; these two parameters basically set the order of magnitude of the maneuver. Impulse size increased linearly as threat radius increased and increased apparently exponentially as maneuver interval shrank. Errors in aiming the interception could reduce the required evasive maneuver to zero, but it was found that errors in the in-track direction did so much more slowly than those along the other axes. After these, the next

most important parameter was orbital altitude. The result that increasing altitude can increase maneuver size by over 50% was not foreseen. Satellite flight path angle also could have a fairly strong effect, but it was only important when the trajectory was nearly vertical. Orbits like these are unlikely in real military satellites. Perhaps the most surprising result was the lack of effect of the interceptor's velocity: changes in direction or magnitude altered the evasive maneuver by only a few percent. The speed of the satellite also had a tactically insignificant effect. Of course, it is unknown if these results are general or if they are peculiar to the case used as a standard. It is also unknown what will happen when two or more of the parameters are varied at once.

Tactics

Many practical aspects of the attack avoidance problem have not been dealt with in this thesis. In a real attack on a satellite, the threat would have to be detected and then tracked for a while to determine its orbit. From this information the defender would deduce the intended target and the time of interception. The defender would have to come to some conclusion regarding the lethal radius of the threat, either from intelligence information or from intelligent guessing. He might decide to defeat the threat by maneuvering, by attacking the attacker, by attacking the enemy's control system, by using chaff or decoys, or by

relying on his satellite's hardening; or he might decide to do nothing and bear the loss. None of this activity has been modeled. However, should the defender decide to attempt an evasive maneuver, the algorithm developed in this research gives him a means of finding the smallest impulse that will evade the threat.

It was found that the required impulse was generally smaller for earlier maneuvers, so it might seem advantageous to maneuver as soon as one has an accurate state vector for the threat. This is the best strategy only if the attacker cannot be retargeted. If the attacker can, an early maneuver may be detected and the interception reestablished by a countermaneuver. The defender might see this and perform another evasive maneuver, but this is a losing game for him: a spacecraft built as an interceptor is likely to have a much larger maneuver capability than one built for another primary mission. He is better off holding his maneuver until there is too little time for the attacker to react to it, providing that his satellite can perform the larger maneuver required.

Even if he could not observe and react to an evasive maneuver, a clever enemy might still defeat it by anticipation. He could calculate his target's optimal evasion, assume that it was going to be made, and plan a last-minute maneuver to nullify it. The attacker could not know the exact maneuver that would seem optimal to the defender: his orbital reductions would give him slightly different

answers and he would not know the exact time of the last-minute evasion. However, he might be able to come close enough. Both spacecraft would then maneuver at about the same time, and the interception would take place before the defender could react. Being aware of this possibility, the defender might choose to make a non-optimal evasive maneuver. The attacker might anticipate this, too. Under these circumstances, the orbital evasion problem becomes the classical military game of trying to outfox the enemy.

Suggestions for Further Work

There are four basic areas for further work on the problem of orbital evasive maneuvers. They are as follows: the performance of the algorithm, the effects of uncertainty, the accuracy of the model, and methods of jointly optimizing maneuver size and other relevant factors. Some comments will be made on each of these.

The only important problem with the algorithm's performance was its slow convergence in certain situations. A method should be found to make the algorithm converge reliably in every situation, without having to guess at a convergence factor. The writer believes that this will prove to be a tractable problem. One approach that might work is to use the existing algorithm to locate the circle on which the optimal solution lies (see Figure 4.2), and then use a different kind of algorithm (bisection, for instance) to find the best point on the circle. If this

problem can be solved, and if computational protection against numerical singularities is added, the existing algorithm should be suitable for tactical use, at least as far as speed and reliability are concerned.

The algorithm in this thesis takes no account of uncertainties in the data, either in knowledge of the state vectors or in the precision with which a recommended maneuver can be made. In a real situation these uncertainties might be large, especially in the knowledge of the attacker's state vector. One response to this problem would be to make the required miss distance large enough to provide protection against all likely variations. However, it might be possible to handle the problem more precisely. One might use the attacker's state and its covariance matrix to find the optimal maneuver that reduces the chance of a successful interception to some acceptable level. There is a similar problem when considering the maneuver. The program as coded calculates evasive maneuvers to tenths of a millimeter per second. If a satellite cannot maneuver this precisely, the uncertainty should be included when the best evasive maneuver is calculated.

The third area for further work is improving the mathematical model of the interception. Two intersting possibilities fall in this area: non-impulsive maneuvers and non-spherical threat volumes. Regarding the former, one might look at evasion with low-thrust electrical rockets as well as at the effect on the evasive trajectory

when supposedly impulsive maneuvers are performed with small station-keeping thrusters. Regarding the latter, one obvious improvement would be to model an attacker with target acquisition device as a conical threat, where the angle of the cone is the field of view of the sensor. The general method of Section II could be applied by writing functions analogous to ρ and ξ (Eqs [2.4] and [2.65]) that measure how close a trial trajectory is to the surface of the cone, and by dividing the problem into cases for passing by the side of the cone, by its base, or by its apex. Of course, this model requires that one have some knowledge of where the attacker will be pointing his sensor.

The last topic that needs to be added to the study of orbital evasion, and perhaps the most important, is that of optimizing other things along with impulse size. As mentioned in the discussion of evasive tactics, it might be very important that the attacker not be able to predict what evasive maneuver will be taken. Now a maneuver the same size as the optimal but in another direction will result in a final position inside the threat sphere. As the maneuver size increases beyond the optimal, the region outside the threat sphere that the satellite might end up in also increases. It would be worthwhile to study how variablity in satellite position increases as the maneuver increases from the smallest that avoids the threat. Another factor that might cause choice of a non-optimal maneuver is

satellite attitude: in some cases the attitude change needed in order to make an optimal maneuver might take too much time, or it might require so much fuel that it would nullify the advantage of making the best maneuver. Furthermore, many satellites can carry out their primary mission only while in one orientation; for them it might be advantageous only to consider maneuvers that require no attitude change or only a small one. Finally, the cost of returning the satellite to its mission orbit has to be considered. The true optimal evasive maneuver is not simply the one that requires the smallest impulse, but rather one that takes into account all of these considerations.

Appendix

Tabulated Results for Variations on the Standard Interception

Tables A.1 through A.11 contain the data that were used to create Figures 5.5 through 5.16. Each table corresponds to one figure, with the exception that Table A.2 was used for both Figure 5.6 and Figure 5.7.

TABLE A.1

Minimum Evasive Impulse vs. Threat Sphere Radius

Radius (km)	Impulse (m/sec)	Radius (km)	Impulse (m/sec)
50	6.6115	550	72.6542
100	13.2215	600	79.2525
150	19.8301	650	85.8499
200	26.4373	700	92.4463
250	33.0433	750	99.0419
300	39.6480	800	105.6368
350	46.2515	850	112.2310
400	52.8538	900	118.8245
450	59.4550	950	125.4175
500	66.0552	1000	132.0098

TABLE A.2

Minimum Evasive Impulse vs. Maneuver Interval

Interval (sec)	Impulse (m/sec)	Interval (sec)	Impulse (m/sec)
500	599.7558	11000	23.1042
1000	299.4778	12000	20.6912
1500	199.2104	13000	18.6614
2000	148.9490	14000	16.9361
2500	118.6936	15000	15.4569
3000	98.4450	16000	14.1794
3500	83.9184	17000	13.0689
4000	72.9718	18000	12.0983
4500	64.4154	19000	11.2456
5000	57.5355	20000	10.4931
6000	47.1410	30000	6.2341
7000	39.6480	40000	4.6606
8000	33.9860	50000	4.0415
9000	29.5592	60000	3.8274
10000	26.0086	70000	3.8142
		80000	3.9320

TABLE A.3

Minimum Evasive Impulse vs. Attacker Speed

Speed (km/sec)	Impulse (m/sec)	Speed (km/sec)	Impulse (m/sec)
0.25	39.6743	2.75	39.4789
0.50	39.6689	3.00	39.4602
0.75	39.6603	3.25	39.4438
1.00	39.6480	3.50	39.4259
1.25	39.6313	3.75	39.4132
1.50	39.6101	4.00	39.4050
1.75	39.5850	4.25	39.4003
2.00	39.5573	4.50	39.3983
2.25	39.5290	4.75	39.3982
2.50	39.5022	5.00	39.3996

TABLE A.4

Minimum Evasive Impulse vs. Attacker Orbital Inclination

Inclination (degrees)	Impulse (m/sec)	Inclination (degrees)	Impulse (m/sec)
0	39.6615	180	39.6854
15	39.6588	195	39.6842
30	39.6530	210	39.6805
45	39.6480	225	39.6749
60	39.6464	240	39.6679
75	39.6485	255	39.6605
90	39.6536	270	39.6536
105	39.6605	285	39.6485
120	39.6679	300	39.6464
135	39.6749	315	39.6480
150	39.6805	330	39.6530
165	39.6842	345	39.6588

TABLE A.5

Minimum Evasive Impulse vs. Attacker Flight Path Angle

Angle (degrees)	Impulse (m/sec)	Angle (degrees)	Impulse (m/sec)
0	39.6480	180	39.6749
15	39.8934	195	39.5566
30	40.1854	210	39.4742
45	40.4545	225	39.4211
60	40.6428	240	39.4000
75	40.7232	255	39.3997
90	40.6977	270	39.4068
105	40.5867	285	39.4098
120	40.4179	300	39.4038
135	40.2199	315	39.3982
150	40.0178	330	39.4209
165	39.8314	345	39.4952

TABLE A.6

Minimum Evasive Impulse vs. Satellite Speed

Speed (km/sec)	Impulse (m/sec)	Speed (km/sec)	Impulse (m/sec)
1.6	39.0954	3.0	39.6162
1.8	39.1552	3.2	39.7015
2.0	39.2219	3.4	39.7875
2.2	39.2941	3.6	39.8737
2.4	39.3705	3.8	39.9598
2.6	39.4501	4.0	40.0454
2.8	39.5323	4.2	40.1302

TABLE A.7

Minimum Evasive Impulse vs. Satellite Flight Path Angle

Angle (degrees)	Impulse (m/sec)	Angle (degrees)	Impulse (m/sec)
0	39.6480	180	39.6749
15	38.6477	195	40.5786
30	38.2409	210	41.3856
45	38.9451	225	42.0946
60	41.6596	240	42.7054
75	47.5959	255	43.2075
90	47.8009	270	43.5705
105	39.4381	285	43.7316
120	36.7093	300	43.5921
135	36.7607	315	43.0675
150	37.6237	330	42.1328
165	38.6734	345	40.9047

TABLE A.8

Minimum Evasive Impulse vs. Satellite Orbit Radius

Radius (km)	Impulse (m/sec)	Radius (km)	Impulse (m/sec)
12000	30.8301	48000	40.5771
16000	27.3967	52000	41.0243
20000	29.5029	56000	41.3657
24000	32.2867	60000	41.6296
28000	34.7389	64000	41.8361
32000	36.6662	68000	41.9996
36000	38.1153	72000	42.1306
40000	39.1889	76000	42.2365
44000	39.9840	80000	42.3231

TABLE A.9

Minimum Evasive Impulse vs. Intercept Radial Miss Distance

Distance (km)	Impulse (m/sec)	Distance (km)	Impulse (m/sec)
-250	6.6153	50	33.0913
-200	13.2290	100	26.4735
-150	19.8406	150	19.8542
-100	26.4493	200	13.2351
-50	33.0535	250	6.6169
0	39.6480		

TABLE A.10

Minimum Evasive Impulse vs.
Intercept In-track Miss Distance

Distance (km)	Impulse (m/sec)	Distance (km)	Impulse (m/sec)
-250	34.4219	50	39.1766
-200	36.2802	100	38.3084
-150	37.7758	150	37.0563
-100	38.8429	200	35.4364
-50	39.4825	250	33.5032
0	39.6480		

TABLE A.11

Minimum Evasive Impulse vs.
Intercept Cross-track Miss Distance

Distance (km)	Impulse (m/sec)	Distance (km)	Impulse (m/sec)
-250	9.0489	50	36.9098
-200	16.2059	100	30.3795
-150	23.3480	150	23.2474
-100	30.4588	200	16.1103
-50	36.9196	250	8.9814
0	39.6480		

Bibliography

1. Bate, Roger R., Donald D. Mueller, and Jerry E. White. Fundamentals of Astrodynamics. New York: Dover Publications, Inc., 1971.

2. Kaplan, Marshall H. Modern Spacecraft Dynamics and Control. New York: John Wiley & Sons, Inc., 1976.

3. Prussing, J. E., and W. G. Heckathorn. "Optimal Impulsive Time-fixed Direct-ascent Interception," paper AAS 85-437 presented at the AAS/AIAA Astrodynamics Specialist Conference, Vail, CO, 12-15 August 1985.

4. Wiesel, William E. Lecture materials distributed in MC 636, Advanced Astrodynamics. School of Engineering, Air Force Institute of Technology (AU), Wright-Patterson AFB, OH, January 1985.

VITA

Captain Roger C. Burk was born on 10 November 1953 in Oakland, California. He graduated from high school in Richmond, California, in 1970 and attended St. John's College in Annapolis, Maryland, from which he graduated cum laude in 1974. He entered the U.S. Civil Service in 1975 and served as a computer programmer for the U.S. Army Computer Systems Command in Falls Church, Virginia, until 1977. He was a graduate student of astronomy at the University of Maryland, College Park, during the academic year 1977-78, and was commissioned in the U.S. Air Force upon graduation from Officer Training School in September 1978. After training as an orbital analyst, he was assigned to the Air Force Satellite Control Facility, Sunnyvale Air Force Station, California, where he served as a Satellite Command Engineer and a Satellite Operations Director until September, 1982. He then served as a project engineer in the Air Force Plant Representative Office at Lockheed Missiles and Space Company, Sunnyvale, California, until entering the School of Engineering, Air Force Institute of Technology, in May 1984.

Permanent address: 2716 Del Monte Ave.
El Cerrito, CA 94530

UNCLASSIFIED

SECURITY CLASSIFICATION OF THIS PAGE

REPORT DOCUMENTATION PAGE

1a. REPORT SECURITY CLASSIFICATION: UNCLASSIFIED	1b. RESTRICTIVE MARKINGS
2a. SECURITY CLASSIFICATION AUTHORITY	3. DISTRIBUTION/AVAILABILITY OF REPORT: Approved for public release; Distribution unlimited.
2b. DECLASSIFICATION/DOWNGRADING SCHEDULE	
4. PERFORMING ORGANIZATION REPORT NUMBER(S): AFIT/GSO/AA/85D-3	5. MONITORING ORGANIZATION REPORT NUMBER(S)
6a. NAME OF PERFORMING ORGANIZATION: School of Engineering; 6b. OFFICE SYMBOL (If applicable): AFIT/ENY	7a. NAME OF MONITORING ORGANIZATION
6c. ADDRESS (City, State and ZIP Code): Air Force Institute of Technology, Wright-Patterson AFB OH 45433	7b. ADDRESS (City, State and ZIP Code)
8a. NAME OF FUNDING/SPONSORING ORGANIZATION: HQ AFSPACECOM; 8b. OFFICE SYMBOL (If applicable): XPYX	9. PROCUREMENT INSTRUMENT IDENTIFICATION NUMBER
8c. ADDRESS (City, State and ZIP Code): Peterson AFB CO 80914	10. SOURCE OF FUNDING NOS. — PROGRAM ELEMENT NO. / PROJECT NO. / TASK NO. / WORK UNIT NO.
11. TITLE (Include Security Classification): See Box 19	
12. PERSONAL AUTHOR(S): Roger C. Burk, Capt, USAF	
13a. TYPE OF REPORT: MS Thesis; 13b. TIME COVERED: FROM _____ TO _____; 14. DATE OF REPORT (Yr., Mo., Day): 1985 December; 15. PAGE COUNT: 100	
16. SUPPLEMENTARY NOTATION	

17. COSATI CODES			18. SUBJECT TERMS (Continue on reverse if necessary and identify by block number)
FIELD	GROUP	SUB. GR.	Maneuvering Satellites, Orbits, Flight Maneuvers, Space Warfare, Evasion.
22	03		

19. ABSTRACT (Continue on reverse if necessary and identify by block number)

Title: MINIMUM IMPULSE ORBITAL EVASIVE MANEUVERS

Thesis Chairman: Joseph W. Widhalm, Lt Col, USAF
Asssitant Professor, Department of Aeronautics and Astronautics

Approved for public release: IAW AFR 190-1.
LYNN E. WOLAVER
Dean for Research and Professional Development
Air Force Institute of Technology (AFIT)
Wright-Patterson AFB OH 45433

20. DISTRIBUTION/AVAILABILITY OF ABSTRACT: UNCLASSIFIED/UNLIMITED ☒ SAME AS RPT. ☐ DTIC USERS ☐	21. ABSTRACT SECURITY CLASSIFICATION: UNCLASSIFIED
22a. NAME OF RESPONSIBLE INDIVIDUAL: Joseph W. Widhalm, Lt Col, USAF	22b. TELEPHONE NUMBER (Include Area Code): (513) 255-2362 — 22c. OFFICE SYMBOL: AFIT/ENY

DD FORM 1473, 83 APR EDITION OF 1 JAN 73 IS OBSOLETE.

UNCLASSIFIED

SECURITY CLASSIFICATION OF THIS PAGE

ABSTRACT

A threat to a satellite is modeled as a sphere of a given radius. The satellite may be required to be outside of the sphere at a given time or never to enter the sphere at all. The threat sphere may be inertially fixed or may move in a keplerian orbit. A method is described of finding the smallest impulsive maneuver that can be made at a given time to avoid the threat. Using the linearized relationship between the satellite state vector at the maneuver time and the state at the intercept time, iterative algorithms are developed that converge on the optimal evasive maneuver. A computer program that implements the algorithms is described. The results of the algorithm are given for several cases. An interception taken from a plausible real-world scenario is used as a basis for investigating how maneuver size varies with the geometry of the interception. (THESIS), K[illegible]